Politecnico di Torino

Politecnico di Torino

Department of Mechanical and Aerospace Engineering

Master of Science in Aerospace Engineering

A.Y. 2023/2024

Conceptual design methodology for commercial supersonic aircraft exploiting drop-in fuels

Supervisor: Davide Ferretto

Co-supervisors Roberta Fusaro
Nicole Viola

Candidate: Riccardo Paternò

Contents

Abbreviations

MORE&LESS	*MDO and REgulations for Low-boom and Environmentally Sustainable Supersonic Aviation*
ICAO	International Civil Aviation Organization
ASTRID	Aircraft on-board Systems sizing and TRade-off analysis in Initial Design
EASA	European Union Aviation Safety Agency
MTOW	Maximum Take-Off Weight
OEW	Operative Empty Weight
SAF	Sustainable Aviation Fuel
SFC	Specific Fuel Consumption
AR	Aspect Ratio
TR	Taper Ratio
MAC	Mean Aerodynamic Chord
SR	Surface Ratio
BFL	Balanced Field Length
NASA	National Aeronautics and Space Administration
ESA	European Space Agency
SBJ	Supersonic Business Jet
QSST	Quiet Supersonic Transport
PMF	Propellant Mass Fraction
AoA	Angle of Attack

Abstract

This thesis work aims to develop a useful analytical method for the preliminary design of a supersonic civil aircraft, within the framework of the European project *MORE&LESS* (*MDO and REgulations for Low-boom and Environmentally Sustainable Supersonic Aviation*). As a matter of fact, subsonic aviation is undergoing rapid and deep developments to be more efficient, characterized by high performance and, most importantly, sustainable. On the other hand, travelling faster than the speed of sound appears necessary to connect people from around the world in an ever-faster way. In such a scenario this project, coordinated by Politecnico di Torino and funded by the European Commission, poses the problem of reviewing the environmental impact of supersonic aviation.

The preliminary high-level analysis is the first step, so the starting point is a database of existing aircraft and a set of theories and equations, all merging in a algorithm implemented in MATLAB environment which, subsequently, allows the user to enter all the inputs needed for calculations and provide intermediate results and graphical outputs. A general overview of what could be some of the most important parameters of the new aircraft is provided from a statistical analysis, whom outputs are needed to the convergence loop of the weight estimation. This step includes mission profile definition and fuel consumption estimation, and it is followed by the main geometry definition, the aerodynamic analysis, and by the verification of take-off and landing requirements according to regulation, as well as of thrust-to-weight ratio and wing surface requirements. In this way the user, at the end of the loop or after any intermediate step, can decide whether to save the obtained results and go on with the detailed analysis, or reject them and start again with different inputs.

The methodology is intentionally specific to Kerosene or Biofuel propellant because, as it will be further discussed in the next section, the aeronautical industries are moving towards reserving liquid hydrogen power to the subsonic aviation, due to the considerable technical difficulties involved in handling liquid hydrogen on board.

At the end the algorithm also allows to run an off-design analysis providing the user with an overview of the impact of initial choices on high-level design: the impact of the number of passengers, range and cruise Mach will be mainly discussed.

SECTION 1

Introduction

The structure of this document reflects the logic flow followed during the development of the method, and it is structured in three sections:

- Section 1 – *Introduction*. In this section the objectives of this thesis work and, in general, the main arguments covered will be introduced.
- Section 2 - *Theoretical Foundations and Framework of Methodology*, with the theoretical bases and all the mathematical equations and assumptions considered for the method development, structured to cover the necessary areas to be defined.
- Section 3 - *Case study and algorithm implementation*. This section reflects in its structure the second one but from a functional point of view. In fact, the algorithm flow and working are shown, with particular attention given to the required inputs, generated outputs and main results.
- Section 4 – *Conclusions and boundaries of application*, in which the main results are summarized and the method boundaries of application are defined.

1.1 Supersonic aviation

The desire to bring back supersonic civil aviation stems from several reasons mainly related to time saving as supersonics aircraft can fly faster than the speed of sound, significantly reducing flight times, particularly on long-haul international routes. As example, if a flight from London to New York typically takes around 8 hours on a subsonic plane, it could take half this time on

a supersonic jet. This would make business travel more efficient, reducing downtime during travel.

During the past decades, supersonic civil aviation, represented by the famous Concorde, stopped existing due to a combination of economic, environmental, regulatory, and safety challenges. Firstly, the cost of operating supersonic fleets was extremely high, due to the high fuel consumption and the small passenger capacity; in fact, if the Concorde could carry around 100 passengers, the Boeing 747 already had a four times higher payload capacity. Moreover, the market demand was not favorable because the high-ticket prices making supersonic flight accessible only to executive, business, and generally wealthy travelers. Also, the possible routes were limited to the ones allowed by the sonic boom noises regulations. The increasing concern for the polluting emissions had a role too, because of the environmental impact of the supersonic. Finally, the public opinion safety concerns after the fatal crash of Air France Flight 4590 in July 2000, involving a Concorde aircraft, accelerated the decline of supersonic aviation [1].

Nowadays, significant advancements have been made in aerodynamics, materials science, engine design, and noise reduction technologies: modern supersonic jets are expected to be more fuel-efficient, quieter, and environmentally friendly than their predecessors. In fact, next generation aircraft development is carried out together with the Sustainable Aviation Fuels (*SAF*) studies to fit within the 2050 global climate goals. During the COP21 held in Paris in 2015, it was established to reduce greenhouse gases emission by 45% before 2030 and to reach the net zero emissions by 2050, to keep global warming to no more than 1.5°C (with respect to the 1800 levels) [2].

Different entities predict the increase in commercial aviation volume. Eurocontrol, which periodically publishes a forecast report, enhances as the actual volume of the commercial aviation (intended as number of flights) has now roughly reached the pre-pandemic levels and two of the three proposed scenarios show an increasing trend over the next decade [3].

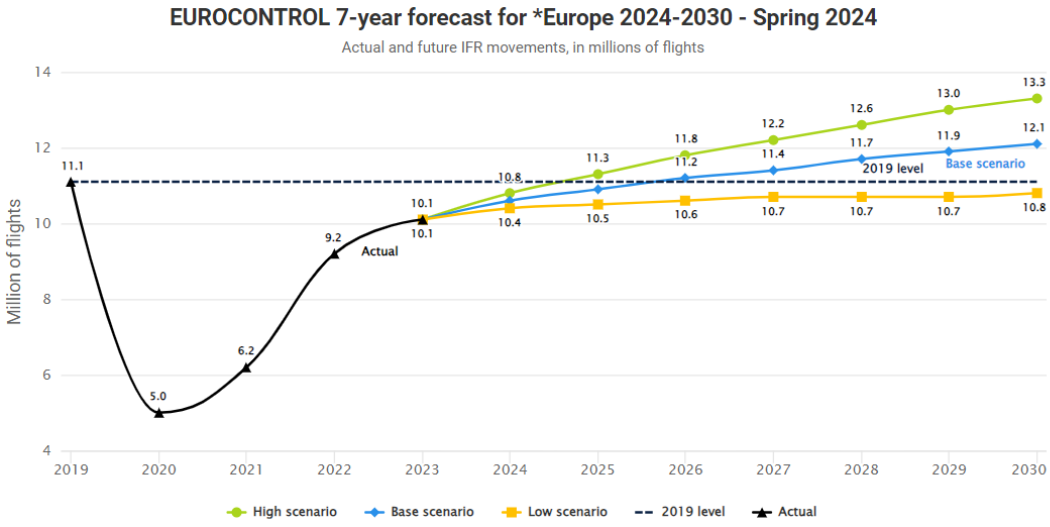

Figure 1.1: 7-year forecast scenarios for European civil aviation [3].

This is a very important aspect to consider when planning how to fit within the globate climate goals: according to previsions, the high-scenario would lead to an increase in the number of flight of over 70%, so only acting with measures as the evolutionary improvement and renewal of the fleets, a better air traffic management and the introduction of alternative propulsive systems, would make possible to reach the *net-zero* level recommended by the Paris agreement [4].

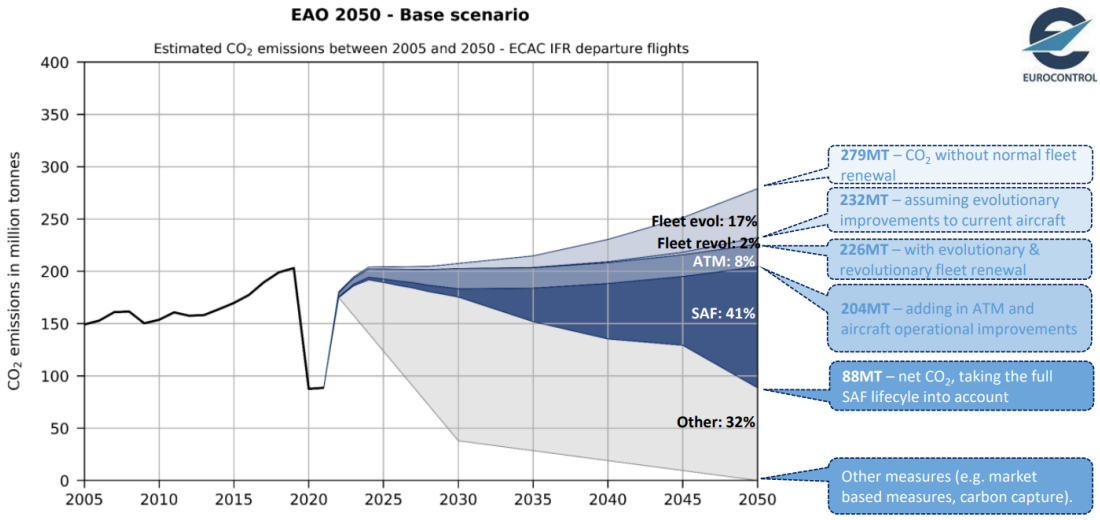

Figure 1.2: CO2 emissions - 2050 scenario [4].

The renewal interest in commercial faster ways of travel perfectly fits in an increasingly interconnected global economy even if, at least at the beginning, the costs would be expensive, thus limiting the supersonic travel again to business and wealthy travelers.

Despite that, studies proved that supersonic civil aviation has now a viable market, with even 500 routes potentially suitable for supersonic flying, especially between Europe, America, Arab Emirates and Australia: by 2035 the market could potentially support around 1000 supersonic airplanes [5].

1.2 MORE&LESS

The international project *MORE&LESS - MDO and REgulations for Low-boom and Environmentally Sustainable Supersonic aviation* [6,7], financed with European funds within the program *H2020* and coordinated by Politecnico di Torino, takes on the challenge to define standards for the development of safe and environmentally friendly supersonic flights. The objectives are in line with *ICAO Assembly Resolution A39-1* [8], which in appendix G and H raises again the question of analyzing the problem of sonic boom and the emission of polluting molecules into the atmosphere and pushes for the scientific fundings in such fields - and in aerodynamics, jet-noise, propulsion, etc. - to be transposed into guidelines for the Regulatory Community. Thanks to the cooperation of sixteen participants, both industries, universities and research centers, widely used and validated software tools for subsonic aviation are enhanced and extended to cover supersonic aviation, to be eventually integrated into the multidisciplinary holistic framework.

Politecnico di Torino finds its place in *task 6.1*: *"Rapid aircraft modelling tool: ASTRID-H 2.0"* [9] through which will be improved the capabilities of *ASTRID-H*, the rapid aircraft modelling tool developed by Politecnico di Torino itself. The work is conceptually divided into three layers:

- *The first layer*: preliminary guess data are provided to initiate the design process. This thesis work fits within this one so it will be discussed in the next chapters.

- *The second layer*: the preliminary estimations are refined based on surrogate models for aerodynamic and propulsive performance, including a preliminary environmental assessment as well.

- *The third layer*: an external validation of the final mission concept will be performed, using the *ASTOS* simulation software.

To start the design process some high-level requirements are needed, such as payload (intended as number of passengers), range, cruise Mach and fuel. The high-level requirements

must be fixed in this phase because the design and methodology choices made from now on will be specifically made to meet those requirements and any change would inevitably lead to a redefinition of the entire process.

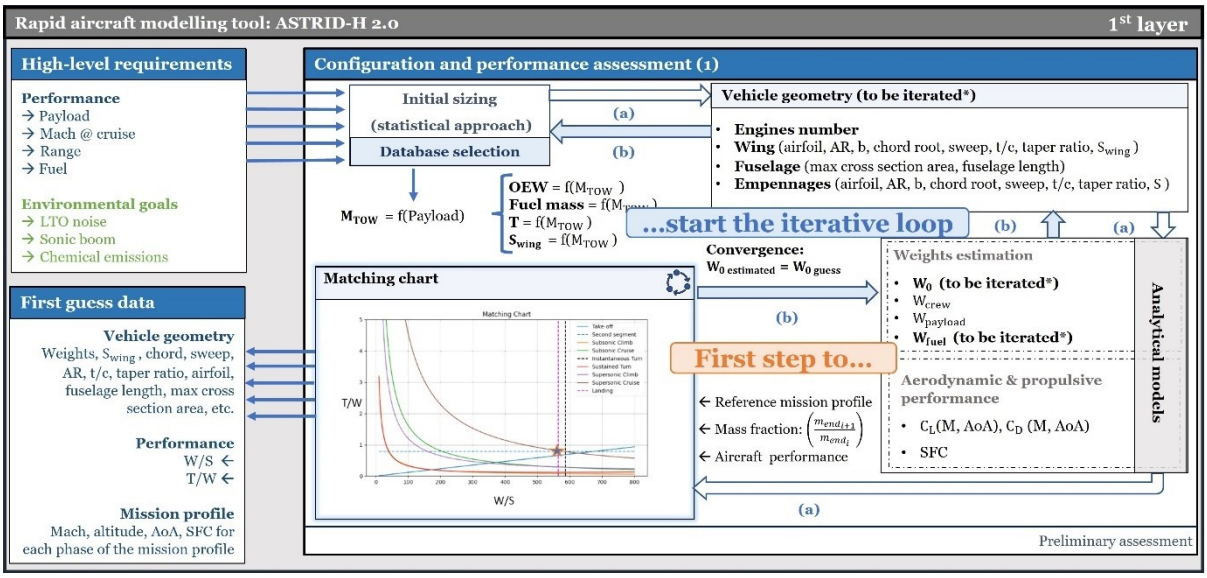

Figure 1.3: ASTRID-H 2.0 logic flow [9].

Once set the high-level mission requirements, the first step is the selection of a database of aircraft with similar performances. This analysis is necessary since, in this early phase, any of the main parameters of case study aircraft is known so a first guess can be carried on through other existing aircraft or case studies.

At this point, empirical mathematical models are used to set, through a convergence loop, the Maximum Take-Off Weight, the fuel weight and the Operative Empty Weight. These data are necessary to define a first draft of the aircraft geometry, especially for what concerns wing and fuselage.

All the information gained since this point are used to build an aerodynamic and propulsive database based on mathematical models. Clearly the analytical approach brings to low fidelity results but again, in this early stage of the design process it would be nearly impossible to make a detailed analysis, which, on the other hand, is the main purpose of the second layer of the *MORE&LESS task 6.1* when aerodynamic and propulsive characterization routine will embed surrogate models based on high-fidelity simulations.

Finally, all the results are collected to perform the requirements verification, not only against the high-level requirements settled at the beginning and the low-level ones raised during the previous steps, but also the ones settled by *EASA* and *ICAO* normative, which are mandatory.

1.3 Case study

Two of the case studies proposed within the *MORE&LESS* program involve a Mach 2 scenario (like Concorde) and a Mach 5 scenario (like Stratofly) [6,9]. While an analytical model could provide a high-level representation of these cases separately within defined boundaries, extending its applicability is challenging due to the significant differences between low-supersonic and hypersonic regimes. Given these variations, introducing a Mach 3 case study would serve as a "bridge" between the two, offering a more continuous progression of analysis. By including a Mach 3 case study, the *MORE&LESS* program can better address the gap between low-supersonic and hypersonic regimes, which are characterized by distinct aerodynamic, thermodynamic, and structural challenges. At Mach 2, the aerodynamics involve manageable shock waves and heating effects, while at Mach 5, the vehicle must contend with extreme thermal loads, shock layer interactions, and complex chemical reactions in the atmosphere.

The high-level requirements for the Mach 3 case study have been set as follows:

High-level requirements	
Cruise Mach	3
Passengers	70
Range [km]	6000
Cruise altitude [m]	18000
Propellant	SAF

Table 1.1: case study high-level requirements.

In this context, the Mach 3 case offers not only a smoother path for developing practical applications like commercial supersonic travel but also a deeper understanding of how to tackle the increasingly severe aerodynamic and thermal challenges as speeds approach the hypersonic threshold.

SECTION 2

Theoretical Foundations and Framework of Methodology

In this section the methodology implemented to start the conceptual design analysis will be described. In fact, despite being still a high-level design, it requires several data input [10].

The output of the statistical analysis is a set of first attempt data, based in the state of art. For this reason, this section is almost user-independent while, as discussed in the following sections, the user can adjust the approach for the calculations to achieve a higher level of detail.

2.1 Statistical analysis

Statistical analysis is the very early starting point of the conceptual design methodology used in this tool as, because of its very nature, the subsequent analyses and convergence loops require specific data input:

- Maximum Take Off Weight (MTOW)
- Operative Empty Weight (OEW)
- Payload weight
- Wing surface
- Thrust
- Propellant Mass Fraction

Taking into consideration a database of existing airplanes or studies designed specifically for the case study, this analysis is a preliminary activity for the next design steps, allowing a first

numerical estimation of those guess data needed to start the conceptual design. Since the results are determined by mathematical interpolation, the output is a guess design point that inevitably reflects the state of art.

The first step is a careful selection of those airplanes or case studies which better fit within the high-level requirements of this case study. The main data determination taking the MTOW as driver parameter follows.

2.1.1 Guess data estimation

In this section the methodology will be discussed considering the MTOW as main driver parameter. Following this approach, a polynomial interpolation is applied to all data from the database taking MTOW as independent variable. The structure of the equations for the 2D case is:

$$f(x) = c_n x^n + c_{n-1} x^{n-1} + \cdots + c_1 x + c_0$$

Where n is the degree of the polynomial. The 3D case is obviously derived from the 2D one.

Each case has been specifically analyzed in order to determine the best approach for the interpolation. In general, since the objective of the analysis is to calculate a regression curve for each parameter, the chosen method is the polynomial interpolation. The interpolation is not always linear, but the polynomial degree is set optimizing the determination coefficient R^2 without badly conditionate the polynomial and maintaining a sensate trend (i.e. monotonous trend).

As mentioned above, particular focus was given to the “construction” of the database. In fact, the definitive set of case studies involved in the calculation was frozen only after verifying that each of them, despite having features which meet the high-level requirements, did not adversely affect any interpolation.

The set of equations obtained, for all the variables analyzed, is the following:

$$MTOW = f(payload)$$

$$S_w = f(MTOW)$$

$$b = f(MTOW)$$

$$Length = f(MTOW)$$

$$PMF = f(MTOW)$$

$$Thrust = f(MTOW)$$

The payload-weight interpolation does not include the MTOW as independent variable. This choice has two reasons, all user oriented. Firstly, it is easier for the user to set the number of passengers as a first input parameter than the MTOW. Furthermore, the guess design point obtained at the end of the statistical analysis is shown in a MTOW vs payload weight graph, together with the result of the subsequent weight estimation: in this way it is clear to the user how near (or far) the design point resulting from the overall high-level design is from the trend calculated by statistical analysis.

Another point of attention is the thrust calculation, as two approaches can be carried out. The first option is to interpolate the thrust data as function of the only MTOW or the only Mach number, the easier one but could offer a limited view. In fact, the net thrust required to the propulsive system to be developed depends at first on both, and moreover the equations applied for the requirement verification see the effect of Thrust, MTOW and speed. For these reasons a 3D interpolation was chosen.

Overall, the logical flow of the process is shown in figure 3.13, with the expected outputs of the analysis.

2.1.2 Second approach

The previous analysis has been conducted considering, as discussed, MTOW as the main driver parameter. However, this is not the only possible approach. As a matter of fact, a stakeholder analysis carried out during the early feasibility study may show the importance of another variable, or simply the user may find useful to calculate the guess design point by controlling another parameter rather than the MTOW (and the number of passengers). For this reason,

the algorithm has been diversified, giving the user the possibility to choose between different strategies:

- Set the MTOW (and the passenger's number) as driving parameter;
- Set the Mach number as driving parameter.

These three options reflect the three main high-level mission requirements, opening to the possibility of performing an off-design analysis studying the sensitivity of the overall preliminary design with respect to those requirements (see Section 4).

All the considerations made above for the data interpolation remain valid, deciding case-by-case the most appropriate polynomial degree.

2.1.3 Outputs definition

The methodology discussed in previous sections was implemented in a MATLAB code in such a way that the user can receive, as output, not only the regression curves calculated through the polynomial interpolation, but also the specific guess design point related to the input parameters. To perform this, the equations are in an iterative loop in which, depending on the selected approach, the passenger number or the Mach number can vary between minimum and maximum values. The results obtained were interpolated with the same considerations as the previous ones, so that the user faces three strategies:

- Choose the passengers number as driving parameter.
- Choose the Mach number as driving parameter.
- Choose a combination of the two above.

Once the driving parameter is set, the guess design point is specifically determined by interpolation with the chosen one as independent variable. If the user selects the third option, he can assign a weight to each of them to consider different aspects but not with the same importance.

The two positive sides are clear: there is the possibility to conduct an analysis which better meets the needs because not always setting the passengers number is the best option, since a stakeholder analysis may result in one (or more than one) another parameter as driver for

the project. On the other hand, the tool offers the possibility to run an off-design analysis being the further calculations dependent on the output obtained at this stage.

Finally, after the selection of one of the approaches above, the guess-data design point is shown.

2.2 Mission profile

The definition of a customized mission profile is needed to perform more detailed analysis, especially for what concerns fuel consumption, as the chosen method for the calculation has a deep dependence on several parameters for each phase of the mission. The phases have been identified considering a generic mission profile for a commercial supersonic aircraft:

1. Warm-up and taxi
2. Take-off
3. Subsonic climb
4. Subsonic cruise
5. Supersonic climb
6. Supersonic cruise
7. Supersonic descent
8. Subsonic descent
9. Missed approach (divided into climb, cruise and descent)
10. Final approach and landing
11. Taxi out

For each phase a set of data must be fixed.

Chosen by the user:

- Distance travelled
- Mach number
- Final altitude reached

Calculated:

- Phase speed:

$$V = M \cdot a$$

  Where M is the phase Mach number and a is the speed of sound.

- Duration:

$$t = \frac{D}{V}$$

  With D being the phase distance and V the average phase speed.

- Atmospheric parameters (pressure, density, temperature and speed of sound), calculated with the International Standard Atmosphere (ISA) model.

Defining a customized mission profile is also important to calculate the total travelled distance, which must meet the range requirement set before. Moreover, all the other analyses performed by the tool become deeply specific for the user case, which clearly brings to a more reliable conceptual design.

For what concerns the take-off and landing phases, at first instance they are managed by the user as the other ones. Eventually, at the end of the preliminary design, the requirements verification is carried on even for what predicted by normative in matter of these two phases, so that distances and speeds are corrected.

2.3 Weights estimation

In this chapter the methodology used for the calculation of the MTOW will be discussed [10]. It can be seen as the sum of different contributions:

$$MTOW = W_{pay} + OEW + W_f + W_{crew}$$

Where:

- OEW is the Operative Empty Weight.
- W_f is the fuel weight.
- W_{pay} is the payload weight.
- W_{crew} is the crew weight.

With payload and crew weights expressed as fixed values, the calculation of the fuel weight and the operative empty weight appear challenging at this stage of the project. For this reason, several methods have been developed but, for their features, only two of them were selected and analyzed within this work: the *Torenbeek* method and the *Raymer* method, and eventually only one selected, being the most suitable.

The OEW is a critical factor as, together with the fuel weight, must be put in a loop that eventually will converge in the final MTOW value. Due to the lack of information regarding others existing aircraft or case studies, this parameter has not been analyzed within the statistical analysis, but it is directly calculated in this section following the two methods mentioned above.

2.3.1 Torenbeek method

This approach was originally developed for subsonic jetliners, but the basic method is applicable to supersonic aircraft as well, having the various terms been calibrated to represent supersonic commercial aviation [11].

Operative Empty Weight

According to this method, the breakdown of the OEW assumes that the MTOW, the Payload weight and the installed take-off thrust are the primary components influencing the OEW:

$$OEW = C_{sys}\left(C_{pay}W_{pay} + C_{af}WMTO\right) + C_{pp}T_{to} + C_{sys} + W_{fix}$$

The bracketed term is called “body group” and represents the fuselage weight, which is primarily determined by the fuselage dimensions and the maximum number of seats in the passenger cabin. This category also includes additional components as equipment and cabin furnishing. If present, the structural weight of the vertical tail size is also classified as a body group weight component, its size being largely influenced by the fuselage geometry and cabin configuration.

- W_{pay} and C_{pay} are respectively the Payload Weight and the Payload coefficient which, for subsonic single-deck aircraft fuselages, depends on the number of side-by-side seats in the main cross-section.

- $C_{af} * WMTO$ is the Airframe Weight, computed respect to the *MTOW* since defining the critical loading condition. This category typically includes the wing structure and the landing gear, as their weights are functionally and statistically proportional to the *MTOW*.

- $C_{pp}T_{to}$ is the installed power plant weight, which amounts to typically 30% of the total installed thrust.

- C_{sys} is the term that accounts on-board power systems such as the environmental control system, hydraulic and electrical generation and flight controls. This factor highlights that the system’s weight, as well as the *MTOW*, depends on the cabin geometry.

- W_{fix} is the Fixed Equipment Weight, all those items present in all commercial aircraft, independent of their size and flight speed.

For the specific case-study the method sets all the above-mentioned parameters as follows:

OEW parameters definition	
C_{pay}	1.50
C_{af}	0.24
C_{pp}	0.125
C_{sys}	0.11
W_{fix}	500 kg

Table 2.1: OEW parameters definition.

Fuel weight

The formulation for the fuel required to fly the design mission is reported in the equation

$$\frac{W_{f,miss}}{MTOW} = \frac{R_{eq}}{P_{cr}R_H + 0.5R_{eq}}$$

In which:

- R_H is the reference range, defined as the ratio between the calorific value of fuel per unit of mass and the gravity acceleration. This parameter, through the calorific value, considers the chosen type of propellant.

$$R_H \stackrel{\text{def}}{=} \frac{H}{g} \approx 4365\ km$$

- P_{cr} is the flight efficiency:

$$P_{cr} \stackrel{\text{def}}{=} \eta_0 \frac{L}{D}$$

  As shown in the equation, it is affected by the aerodynamic and propulsive features of the aircraft. Propulsive efficiency depends on the propellant as well through the specific impulse and calorific energy per unit of mass.

- R_{eq} is the equivalent all-out range, as shown in the equation

$$R_{eq} = R_{des} + R_{lost} \approx R_{des} + 0.2R_H$$

Where R_{lost} takes account for the additional fuel needed to take into account the other non-cruises phases of the mission and the additional fuel required for maneuvering. Since the method is based on the assumption of quasi-stationary flight during cruise, the generalized Breguet's equation can be applied:

$$R = R_H P_{cr}\, ln\left(\frac{MTOW}{W_{final}}\right)$$

Where R is the design cruise range. The formulation reported above brings to the 0.5 factor in the fuel equation, deriving from a Fourier series approximation of the natural logarithm. From a "practical" point of view, it means that the average specific range is assumed to be equal to the nominal specific range when half of the cruise fuel has been consumed.

W_{final} is the final weight of the aircraft. It is computed as the sum between the Maximum Zero Fuel Weight (assumed as $0.5 \cdot MTOW$) and the reserve fuel, assumed proportional to the *MTOW* according to the equation

$$W_{res} = C_{res} MTOW = 0.0065 * MTOW$$

Both OEW and fuel weight are computed within a convergence loop on the MTOW.

2.3.2 Raymer method

Operative Empty Weight

According to the Raymer's method, an exponential equation describes the relationship between the OEW and the MTOW [12]:

$$\frac{OEW}{WMTO} = k_{mat} k_{sw} A * MTOW^{C}$$

Proper sets of the coefficients A and C present in the equation define different aircraft categories, while the two others refer to the material adopted and to the wing sweep type.

Category	A	C
Sailplane – unpowered	0.86	-0.05
Sailplane – powered	0.91	-0.05
Homebuilt – metal/wood	1.19	-0.09
Homebuilt – composite	0.99	-0.09
General aviation – single engine	2.36	-0.18
General aviation – twin engine	1.51	-0.10
Agricultural aircraft	0.74	-0.03
Twin turboprop	0.96	-0.05
Flying boat	1.09	-0.05
Jet trainer	1.59	-0.10
Jet fighter	2.34	-0.13
Military cargo/bomber	0.93	-0.07
Jet transport	1.02	-0.06

Table 2.2: A and B coefficients for different airplanes categories.

k_{mat}	1	Metallic structure
	1.04	Composite structure
k_{sw}	1	Fixed sweep
	1.04	Variable sweep

Table 2.3: material coefficients.

Fuel weight

Raymer's method for the fuel weight calculation is based on the ratio between the final and initial mass of the aircraft for each phase of the mission thus, for each one of them, the Breguet equation is applied.

$$\frac{W_i}{W_{i-1}} = exp\left(\frac{-R * SFC}{V * E}\right)$$

According to the method, for some phases the ratio assumes a constant value, while for others it must be calculated. These phases are warm-up and take-off, subsonic climb and landing:

$$\frac{W_i}{W_{i-1}} = \begin{cases} 0.97 \rightarrow Warm - up \\ and\ taxi \\ \\ 0.985 \rightarrow Subsonic \\ climb \\ \\ 0.995 \rightarrow Landing \end{cases}$$

The parameters present in the equation are listed below:

- R is the distance travelled within the analyzed mission phase, determined through the user input as follows

  $$R = V \cdot t$$

  Where t is the duration of the phase.

- V is the aircraft average speed as computed from the Mach number set by the user, with the information regarding the phase altitude.

- SFC is the Specific Fuel Consumption. It does not depend only on the used propellant but also on the engine itself so, unless the engine to be used is known with its technical features, this is a very difficult parameter to estimate at this stage of the design.

- E is the aerodynamic efficiency calculated as C_L/C_D. This value normally comes from aerodynamic analysis, but it has not been performed yet. For this reason, at this early stage, the aerodynamic efficiency value was estimated to be a constant value. At the end of the process this (and other parameters) will be updated, and a second iteration of the entire loop will be run.

2.3.3 Chosen approach

Both methods were implemented with the following results:

	Torenbeek	**Raymer**
$MTOW\ [kg]$	16447.39	70785.63
$W_{fuel}\ [kg]$	4558.95	24520.5
$OEW\ [kg]$	2487.86	37365.13
$\frac{OEW}{MTOW}$	0.15	0.53

Table 2.4: Torenbeek-Raymer results comparison.

It is evident that the difference between the two approaches is large, with the *Torenbeek* method that tends to underestimate the fuel and the operative empty weights. Having analyzed both methods, some considerations were made. The *Torenbeek* one is specifically taught as a guideline for the supersonic commercial aircraft conceptual design; therefore, it appears at first sight as the most suitable method. On the other hand, the fact that it is independent from the mission profile and the uncertainty caused by the large number of empirical coefficients in its formulation, led to the Raymer method's final choice. Raymer method, indeed, has a simple but effective operative empty weight formulation and a detailed fuel weight estimation.

During the development of this tool, the choice not to consider as constant the weight ratio during warm-up and take-off, subsonic climb and landing phases was considered because, despite the impact of a higher level of detail for these phases is low if compared to the cruise phase, applying the Breguet equation to these ones as well does not increase the complexity of the analysis. Furthermore, such an approach fits well with the implementation of the algorithm into a convergence loop. This aspect will be discussed in detail in Section 3.

The critical point for the *Raymer* method application is, as previously mentioned, the Standard Fuel Consumption (SFC) estimation. For this case study the approach for this aspect was to set a reference SFC derived from the state-of-the-art of the hydrocarbon propelled turbofan propulsors and to scale it to consider the possibility of a Sustainable Aviation Fuel (SAF):

$$SFC = \frac{H_{ref}}{H_{saf}}\, SFC_{ref}$$

As shown in the equation, since the propulsor specifications are unknown at this stage, the only parameter used is the ratio between the two calorific energies per unit of mass. In addition, for each phase of the mission the SFC was further scaled in order to consider the differences between them which led to different fuel consumption. The variables used for this scope were throttle and altitude, and literature suggests the semi-empirical approach:

$$SFC = \phi * \varphi *\ SFC_{ref}$$

$$\phi = \frac{\Pi_{phase}}{\Pi_{cruise}} \qquad \varphi = \frac{p_{phase}}{p_{sl}}\left(\frac{T_{sl}}{T_{phase}}\right)^{1.75}$$

Where p and T are the atmospheric pressure and temperature.

2.4 Aerodynamic analysis

Aerodynamic analysis is the subsequent step of the conceptual design, for which the methodology is discussed in this section. The main purpose is to determine the aerodynamic database, specific for the case study and the input parameters set by the user. The parameters which must figure in such a database are:

- Lift coefficient (C_L)
- Drag coefficient (C_D)
- Aerodynamic efficiency (E)

The determination of these three parameters requires the definition of a large set of geometric and aerodynamic data, as shown in this chapter. Since the main purpose of the *MORE&LESS* project at this stage is to merge a coherent set of theories and methods into a tool which, starting from a series of inputs, brings to a design point through analytical calculations, the aerodynamic database is not derived from experimental results, but it is analytically computed. Only as the last step algorithm validation through a more detailed numerical analysis be discussed.

The following approach was derived from the Raymer method [12]. The reasons that led to this choice were mainly related to the high level of confidence gained in the output results, including also calculations for the transonic flight regime. On the other hand, the knowledge of a large set of input data is mandatory and the algorithm flow is complex, that may result in performances decrease for the overall program flow.

In the following sections the methodology will be implemented for the calculation of both the lift and the drag coefficients. For the calculations, the cases have been distinguished, depending on the flight regime:

- Subsonic: Mach < 0.8
- Transonic: Mach between 0.8 and 1.2
- Supersonic: Mach between 1.2 and 5.

The definition of the transonic flight regime finds its reasons in the fact that, despite the actual aircraft speed is subsonic, locally the flow can reach a Mach number greater than 1 because

of the surface's curvature. On the other hand, even when the aircraft speed is lightly supersonic, locally the flow can still be characterized by a subsonic regime. On the other hand, Mach 5 is the upper limit of the supersonic flight, beyond which the flight regime is hypersonic, eluding from this analysis.

2.4.1 Lift coefficient calculations

The main assumption is that the relationship between the lift coefficient and the angle of attack is linear:

$$C_l = C_l\alpha$$

This may be considered true for low angles of attack and, in general, far from the stall conditions.

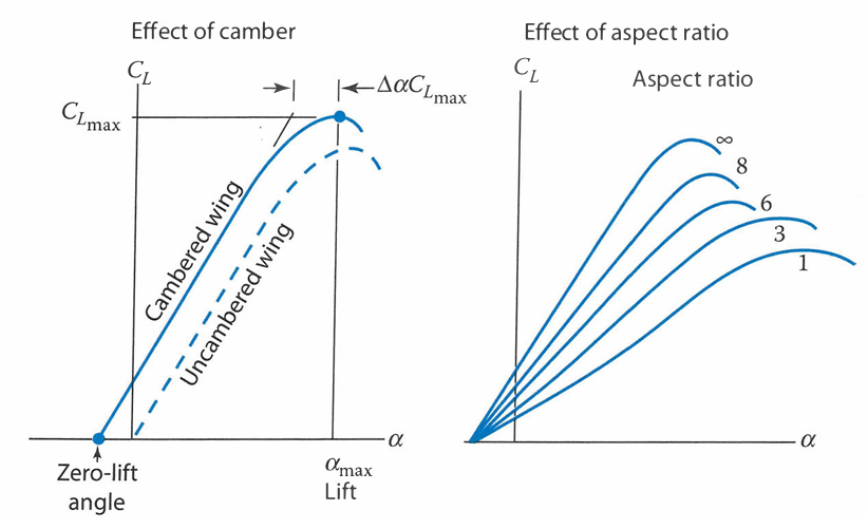

Figure 2.1: C_L-α curves [12].

Subsonic regime

The subsonic regime of flight is considered as the one for which the Mach number is lower than 0.8. In this regime the $C_{l,\alpha}$ slope coefficient is computed through the equation:

$$C_{L\alpha} = \frac{2\pi \cdot AR}{2 + \sqrt{4 + \left(\frac{\beta * AR}{\eta}\right)^2 \left(1 + \frac{tan\,\Lambda}{\beta}\right)^2}} \cdot SR \cdot F$$

Where:

- AR is the aspect ratio, defined as the ratio:

$$AR = \frac{b^2}{S_w}$$

  Being b the wingspan and S_w the wing surface.

- β is a parameter defined by the expression

$$\beta = \sqrt{1 - M_{cr}^2}$$

  Being M_{cr} the Mach number during the subsonic cruise.

- Λ is the radiant wing sweep angle.

- η is the airfoil efficiency, derived from literature for this case study.

- F is the fuselage lift factor, defined by the expression

$$F = 1.07 \cdot \left(1 + \frac{d_{fus,ext}}{b}\right)^2$$

  $d_{fus,ext}$ is the external diameter of the fuselage.

- SR is the surface ratio, defined as

$$SR = \frac{S_{exp}}{S_{ref}}$$

  Where S_{exp} is the wing reference area without the portion of the wing covered by the fuselage, and S_{ref} is the planform or reference area.

In this case, the wing reference area is derived from statistical analysis, while the portion of the wing covered by the fuselage is considered to be rectangular, given the root chord of the wing and the fuselage diameter.

Supersonic regime

The supersonic regime of flight is considered as the one for which the Mach number is greater than 1.2 and lower than 5. In this regime of flight, the equation for the $C_{l,\alpha}$ modifies as follows:

$$C_{L\alpha} = \frac{4}{\sqrt{1 - M^2}}$$

This equation is valid only if the leading edge of the wing has entered the supersonic regime: this means that must be verified the expression

$$M > \frac{1}{cos\ \Lambda_{le}}$$

Which means that the Mach cone is greater than the wing sweep angle.

Transonic regime

The transonic regime of flight is considered as the one for which the Mach number is between 0.8 and 1.2. The algorithm for this section was implemented to build a "smooth curve" between the two regimes, since none of the two analytical approaches is valid in this region. The chosen strategy was to compute beta, F, $C_{L\alpha}$ and C_L for both Mach numbers (0.8 and 1.2), for the first case applying the subsonic regime method and for the second case the supersonic one. Then, a polynomial interpolation was made between the obtained values, thus giving continuity to the curve determined from the subsonic regime to the supersonic, passing from the transonic regime of flight.

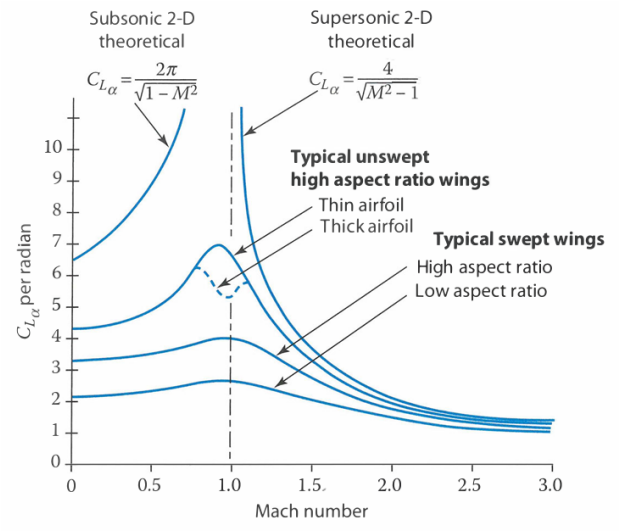

Figure 2.2: C_L-Mach curves [12].

2.4.2 Drag coefficient calculations

The approach for the calculation of the drag coefficient is the same as shown for the lift coefficient, splitting the calculation between the three flight regimes.

Subsonic regime

The equation considered for the subsonic flight regime is:

$$C_D = C_{D0} + C_{D,i}$$

Which sees the contribution of the parasite drag and of the drag due to lift.

PARASITE DRAG

$$C_{D0} = \frac{\sum\left(C_{f,i} \cdot FF \cdot Q_i \cdot S_{wet}\right)}{S_{ref}} + C_{D,misc} + C_{D,lp}$$

$C_{D,misc}$ is the miscellaneous drag term. It considers all the non-streamlined objects exposed to the flow. The calculation was made for the base area and flaps. The base area is intended as any aft-facing flat surfaces, any place where the aft fuselage angle to the freestream exceeds about 20°.

$$C_{D,misc,flap} = 0.002 \cdot \frac{b_{flap}\delta_{flap}}{b}$$

$$C_{D,misc,basearea} = \frac{\left(0.139 + 0.419(M - 0.161)^2 \cdot S_{flap}\right)}{S_{exp}}$$

Where the introduced parameters are:

- b_{flap} is the flaps span.
- δ_{flap} is the flaps deflection angle.
- b is the wingspan.
- S_{flap} is the flaps surface.

$C_{D,lp}$ term accounts the protuberances effects (hinges for the control surfaces, antennas, rivets heads, misalignment of the panels) and leakages caused by gaps, for which the aircraft has the

tendence to increase resistance in the high-pressure areas and to facilitate the flow separation in the low-pression areas. The contribution is accounted as 2% to 5% of the total parasite drag.

$C_{f,i}$ is the skin friction drag, calculated for wing, fuselage, vertical tail (if present), horizontal tail, canard (if present), nacelles and jet inlets.

At first the Reynolds number must be calculated to determine the flow regime, if laminar or turbulent.

$$Re = \frac{\rho V l}{\mu} \quad \begin{cases} < 1.5 \cdot 10^5 \rightarrow laminar\ flow\ regime \\ > 1.5 \cdot 10^5 \rightarrow turbulent\ flow\ regime \end{cases}$$

Where l is defined as the Main Aerodynamic Chord (MAC) if considering the wing or the tail, or defined as the length if considering the fuselage or the nacelle. The Main Aerodynamic Chord is the chord identified at $1/3$ of the half wingspan (if considering the wing) or at $1/3$ of the height (if considering the tail).

$$Position_{MAC} = \begin{cases} {}^1/_3 \cdot {}^b/_2 \\ {}^1/_3 \cdot tail\_height \end{cases}$$

$$MAC = \begin{cases} Position_{MAC} \cdot \dfrac{c_{root}}{{}^b/_2} \\ Position_{MAC} \cdot \dfrac{c_{root}}{tail\_height} \end{cases}$$

Where c_{root} is the root chord.

The calculation of the Cf is different between the two flow regimes:

$$Re_{cutoff} = 38.21 \cdot \frac{l}{k}$$

Where l is defined as the MAC if considering the wing or the tail, $lenght$ if considering the fuselage or the nacelles.

$$C_{f,laminar} = \frac{1.328}{\sqrt{Re}}$$

$$C_{f,turbolent} = \frac{0.455}{log\ Re^{2.58} \cdot (1 + 0.144 \cdot M^2)^{0.65}} \qquad if\ Re < Re_{cutoff}$$

$$C_{f,turbolent} = \frac{0.455}{log\ Re_{cutoff}{}^{2.58} \cdot (1 + 0.144 \cdot M^2)^{0.65}} \qquad if\ Re > Re_{cutoff}$$

Considering the Reynolds number definition, ρ is the atmospheric density, V is the aircraft speed and μ is the dynamic viscosity.

k is the skin roughness value that takes into account the skin roughness of the surfaces, as it affects the regime of the flow. According to Raymer's method, different values must be considered depending on the surface material:

Surface type	$\boldsymbol{k \cdot 10^5}$ $[\boldsymbol{ft}]$
Camouflage paint on aluminum	3.33
Smooth paint	2.08
Production sheet metal	1.33
Polished sheet metal	0.5
Smooth molded composite	0.17

Table 2.5: Skin roughness coefficient.

FF is the pressure or form drag, defined as the contribution to the parasite drag due to the flow separation.

$$FF = \left(1 + \frac{0.6}{x/c} \cdot \frac{t}{c} + 100 \cdot \frac{t^4}{c}\right) \cdot (1.34\ M^2 (cos\ \Lambda)^{0.28}) \qquad \textit{Wing and tail}$$

$$FF = 1 + \frac{60}{f^3} + \frac{f}{400} \qquad \textit{Fuselage}$$

$$FF = 1 + \frac{0.35}{f} \qquad \textit{Engines}$$

Where:

- $\frac{t}{c}$ is the ratio between the profile thickness and the chord.
- x/c is the chordwise location of the airfoil maximum thickness.
- f is the ratio between the length and the diameter of the fuselage and the engine.
- Λ is the sweep angle of the wing or the tail.

Q is term which accounts for the interference drag: it has been shown that the boundary layers of different elements interfere, causing an increase in the parasite drag. Typical values for this term are the ones reported in the next table.

Element	Q
High-wing, mid-wing, well-filleted low wing	1
Undiluted low wing	1.1 – 1.4
Nacelle or external store directly mounted on the fuselage or wing	1.5
Nacelle or external store directly mounted less than one diameter away from the fuselage or wing	1.3
Nacelle or external store directly mounted more than one diameter away from the fuselage or wing	1
Wing-tip mounted missiles	1.25
Conventional tail	1.04 – 1.05
V-tail	1.03
H-tail	1.08

Table 2.6: Interference drag for different elements interfere.

S_{wet} is the wet area. It is, for each considered element, the surface area exposed to the flow.

For the wing, it is sufficient to multiply the exposed surface by four, to consider both upper and lower sides of the wing:

$$S_{wet} = S_{exp} \cdot 4 \cdot \%_{wetteed\_surface}$$

For the tail, the geometry considered is simple enough to allow the direct calculation of its surface. The value obtained shall be multiplied by two to consider both sides of the tail.

$$S_{wet} = S_{triangle} \cdot 2 \cdot \%_{wetteed\_surface}$$

For the fuselage, the wetted surface is the cylinder area:

$$S_{wet} = S_{cilinder} \cdot \%_{wetteed\_surface}$$

For the nacelles, the wetted surface is the cylinder area as well, assuming that those elements have a cylinder-like geometry. Obviously, the obtained value must be multiplied by the number of engines.

$$S_{wet} = S_{cilinder} \cdot n_{engines} \cdot \%_{wetteed\_surface}$$

INDUCED DRAG

The induced drag or drag due to lift considers the increment in the parasite drag caused by the viscous separation, due to the speed gradient around the wing profile:

$$C_{D,lp} = K\, C_L^2$$

Where C_L is the lift aerodynamic coefficient and K is a coefficient, whose formulation must assume two forms: for a wing with a sweep angle lower than 30° the "classical Oswald method" is applied, while for a wing with a sweep angle greater or equal to 30° a more complex "leading edge suction method" shall be considered. However, in this case the classical Oswald method is applied.

In general, the relation for K is:

$$K = \frac{1}{\pi \cdot AR \cdot e}$$

Where AR is the aspect ratio and e is the Oswald factor. The approach for the algorithm implementation was to discriminate for three different cases, depending on the sweep angle.

- $\Lambda < 2°$

$$e = 1.78 \cdot (1 - 0.45 \cdot AR^{0.68}) - 0.64$$

- $\Lambda \geq 30°$

$$e = 1.78 \cdot (1 - 0.45 \cdot AR^{0.68}) \cdot (cos\,\Lambda)^{0.15} - 3.1$$

- $2 \leq \Lambda < 30°$: the Oswald factor was calculated as linear interpolation between the two cases, without committing an appreciable error.

Supersonic regime

The equation considered for the supersonic flight regime is the same as for the subsonic regime, which sees the sum of two drag components but with the appropriate adjustment to consider some elements not present in the previous analysis.

PARASITE DRAG

In order to account for the parasite drag term, the applied relationship is the following:

$$C_{D0} = \frac{\sum(C_{f,i} \cdot S_{wet})}{S_{ref}} + C_{D,misc} + C_{D,lp} + C_{D,wave}$$

While the other terms have the same meaning as for the subsonic case, a new contribution in the calculation of the parasite drag is present, the wave drag.

$C_{D,misc}$, as for the previous case, is the miscellaneous drag term. It considers all the non-streamlined objects exposed to the flow. The calculation was made for the base area and flaps. The base area is intended as any aft-facing flat surfaces, any place where the aft fuselage angle to the freestream exceeds about 20 deg. The equations are lightly different from the previous case:

$$C_{D,misc,flap} = 0.003 \cdot \frac{b_{flap}\delta_{flap}}{b}$$

$$C_{D,misc,basearea} = \frac{\left(0.064 + 0.042(M - 3.84)^2 \cdot S_{flap}\right)}{S_{exp}}$$

$C_{D,lp}$ term accounts the protuberances effects (hinges for the control surfaces, antennas, rivets heads, misalignment of the panels) and leakages caused by gaps, for which the aircraft has the

tendence to increase resistance in the high-pressure areas and to facilitate the flow separation in the low-pression areas. The contribution is accounted as 2% to 5% of the total parasite drag.

The skin friction drag was again calculated for wing, fuselage, vertical tail (if present), horizontal tail, canard (if present), nacelles and jet inlets. Once calculated the Reynold's number in order to determine the flow regime, if laminar or turbulent, the Re cutoff is calculated according to the equation:

$$Re_{cutoff} = 44.62 \cdot \left(\frac{l}{k}\right)^{1.053} \cdot M^{1.16}$$

Then, depending on the flow regime, the C_f term is computed through the relations:

$$C_{f,laminar} = \frac{1.328}{\sqrt{Re}}$$

$$C_{f,turbolent} = \frac{0.455}{log\, Re^{2.58} \cdot (1 + 0.144 \cdot M^2)^{0.65}} \qquad if\ Re < Re_{cutoff}$$

$$C_{f,turbolent} = \frac{0.455}{log\, Re_{cutoff}{}^{2.58} \cdot (1 + 0.44 \cdot M^2)^{0.65}} \quad if\ Re > Re_{cutoff}$$

The wave drag $C_{D,wave}$ is the very peculiar term of the supersonic regime. It includes the effects due to the increment in drag caused by the shock wave formation. It mainly depends on the longitudinal volume distribution of the aircraft.

$$C_{D,wave} = E_{WD} \cdot \left(1 - 0.2 \cdot (M - 1.2)^{0.57} \cdot \left(1 - \frac{\pi \cdot \Lambda}{100}\right)\right) \cdot \left(\frac{D}{q}\right)_{Sears-Haak}$$

Where the term $\left(\frac{D}{q}\right)_{Sears-Haak}$ is the Sears-Haack body wave drag:

$$\left(\frac{D}{q}\right)_{Sears-Haak} = \frac{9}{2}\pi \left(\frac{A_{max}}{l}\right)^2$$

The Sears-Haack body is defined as the volume body which generates the lowest wave drag. Being S the cross-sectional area of a volume distribution, the wave drag is function of the second derivative of the cross-sectional area distribution $S''(x)$. For this reason, the cross-

sectional area distribution $S(x)$ must be as smooth as possible, identical, at the limit, to the Sears-Haack body one.

In this equation, A_{max} is the max cross-sectional area. In an aircraft, A_{max} is defined as the area at the main landing gear location. Literature suggests computing this term considering three contributions, engines, wing and fuselage:

$$A_{fuselage} = \pi \left(\frac{D}{2}\right)^2$$

$$A_{engines} = n_{engine} \cdot \pi \left(\frac{D}{2}\right)^2$$

$$A_{wing} = 0.25 \cdot A_{max}$$

For what concerns the wing, the typical delta wing design for supersonic configurations determines a complex geometry, therefore, as suggested by literature, this contribution was calculated adding 25% at the total value. D is the diameter of the considered element.

E_{WD} is the wave drag efficiency factor, defined as the ratio

$$E_{WD} = \frac{C_{D,wave}}{C_{D,wave,Sears-Haak}}$$

Configuration	E_{WD}
Poor supersonic design	2.5 – 3.0
Blended delta wing	1.2
Supersonic fighter, bomber, SST	1.8 – 2.2

Table 2.7: Wave drag efficiency factor for different wing types.

As shown in the table above, E_{WD} is chosen depending on the configuration.

INDUCED DRAG

As for the subsonic case, the induced drag or drag due to lift considers the increment in the parasite drag caused by the viscous separation, due to the speed gradient around the wing profile.

$$C_{D,lp} = K\, C_L^2$$

For supersonic flight regime the Oswald classical method was considered for the calculation of the K coefficient, with the case adjustments:

$$K = \frac{AR \cdot (M^2 - 1) \cdot cos\, \Lambda}{4 \cdot AR \cdot \sqrt{M^2 - 1} - 2}$$

Transonic regime

The transonic regime analysis is way more complex than the previous analyses. For this reason, considering the high-level design purpose of this tool, it was chosen to interpolate all the results obtained for the subsonic and supersonic cases. Therefore, even if a simplification of the problem was introduced, at least a sort of connection was created between the subsonic regime and the supersonic one, allowing the aerodynamic characterization for this regime of flight as well.

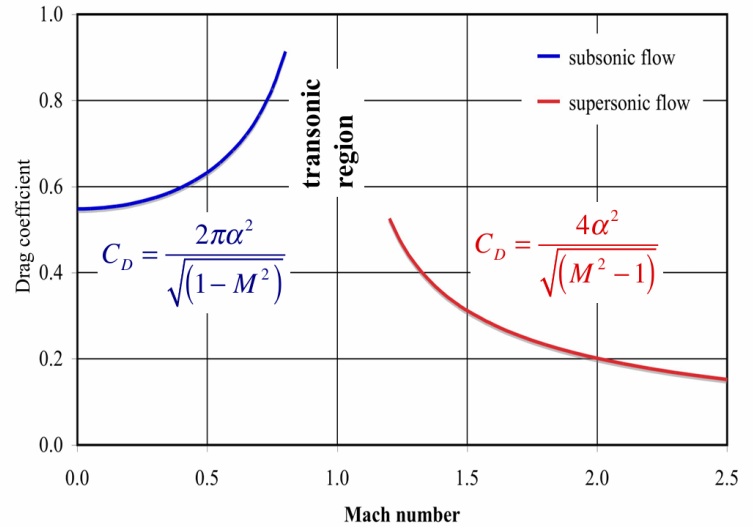

Figure 2.3: Mach-C_D curve.

2.5 Requirements verification

The requirements analysis and verification are the final step of the high-level conceptual design as it verifies the mission and project feasibility, from a technical point of view and an operational one as well.

In this section the methodology implemented for the verification requirements will be discussed. For the purposes of this analysis, “requirements” are intended all the mandatory ones as set by the *CS-25* [13], concerning the take-off and landing phases of flight.

2.5.1 Take-Off analysis

The take-off assessment involves determining two distinct parameters: the standard take-off distance, encompassing ground roll and climb phases, and the Balanced Field Length (BFL), which considers potential single-engine failure scenarios. The certified take-off distance under *CS-25* regulations is determined as the greater value between the BFL and 1.15 times the standard take-off distance. In both scenarios, take-off distance is measured from the commencement of ground roll to surpassing a 35 feet high vertical obstacle. The evaluation of Balanced Field Length follows a similar procedure, necessitating simulation of single-engine failure from speeds ranging from 0 to take-off speed. This involves calculating distances for both continuing the take-off and aborting to a full stop; the speed at which these distances equate is known as the decision speed or *V1*, and the corresponding distance is the BFL. The figure below, sourced from Raymer's referenced work, delineates the various segments of the take-off distance, each of which will be detailed subsequently.

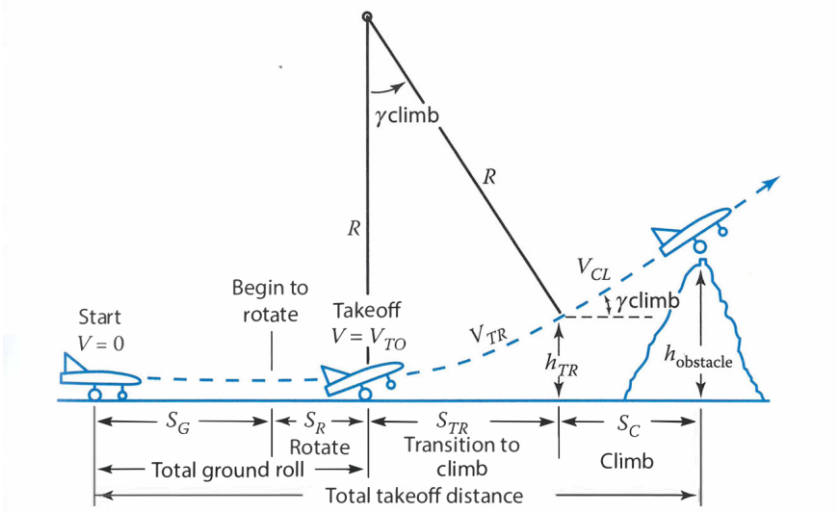

Figure 2.4: Take-Off phases division [12,13].

Here is a summary outlining the different segments and the methodologies utilized to quantify each:

- *Total ground roll*: This segment accounts for the acceleration from rest to take-off speed, which is typically evaluated as 1.1 times the stall speed in the flapped configuration, along with the rotation phase. The general formulations for both acceleration and deceleration phases are as follows:

$$S_G = \frac{1}{2gK_A} ln \frac{K_T + K_A V_f^2}{K_T + K_A V_i^2}$$

where the two coefficients are:

$$K_T = \frac{T}{W} - \mu$$

$$K_A = \frac{\rho}{2 \cdot W/S} (\mu C_L - C_{D0} - K C_L^2)$$

μ is the friction coefficient, relative to the friction between wheels and the runway asphalt. During the acceleration phase, common values for this term are between 0.03 and 0.05 while, during the breaking phase typical values are between 0.3 and 0.5.

T is the thrust, W the Maximum Take-Off Weight, ρ the air density, C_L is a mean value of the lift coefficient during the acceleration, evaluated as

$$C_L = C_{L,take-off} \cdot \sqrt{2}$$

C_{D0} is the parasite drag and, for the term relative to the induced drag, the coefficient K has been evaluated through the relation

$$K = \frac{1}{\pi \, e \, AR}$$

Since this maneuver lasts two to three seconds, the speed can be considered constant to the value $3 \cdot V_{TO}$.

- *Transition to climb phase*: In this phase, the aircraft ascends and accelerates to the initial climb speed, which must be at least $1.2 \cdot V_{stall}$ in the take-off configuration. Thus,

the average value for the velocity can be assumes as $1.15 \cdot V_{stall}$, while the average C_L as 90% the maximum value for the flapped configuration. The average load factor for vertical acceleration can be calculated as

$$n = \frac{L}{W}\frac{{}^1\!/_2\,\rho S\left(0.9C_{L,max}\right)(1.15V_{stall})^2}{{}^1\!/_2\,\rho S C_{L,max}V_{stall}^2} = 1.2$$

However, the vertical load factor must satisfy the following relation, the second term being the centripetal acceleration caused by the circular trajectory followed by the airplane during this phase:

$$n = 1 + \frac{V_{TR}^2}{R_G} = 1.2$$

The two equations are solved for the radius:

$$R = \frac{V_{TR}^2}{g(n-1)} = \frac{V_{TR}^2}{0.2g} \cong V_{stall}^2$$

The climb angle at the end of the transition is evaluated as

$$sin\,\gamma = \frac{T-D}{W} \cong \frac{T}{W} - \frac{1}{{}^L\!/_D}$$

Thus, the horizontal distance traveled, and the altitude gained during transition are calculated, respectively, as

$$S_T = R\,sin\,\gamma = R\frac{T-D}{W} \cong R\left(\frac{T}{W} - \frac{1}{{}^L\!/_D}\right)$$

$$h_{TR} = R(1 - cos\,\gamma)$$

It may happen that the altitude gained by the airplane is enough to clear the obstacle already in this phase. In such a case, there is no need to analyze the following climb stage and the distance travelled can be calculated as:

$$S_T = \sqrt{R^2 - (R - h_{TR})^2}$$

- *Climb*: eventually, the horizontal distance necessary to clear the obstacle depends on the altitude reached at the end of the previous phase:

$$S_C = \frac{h_{obstacle} - h_{TR}}{tan\,\gamma}$$

The BFL is the total take-off distance (including the clearance of the obstacle) in condition of one engine inoperative. The process for the calculation is iterative. For each speed considered for the engine fail, both the take-off run distance, and the breaking distance are calculated. The speed for which the two distances are equal is defined as V1 and the corresponding distance is the BFL. Therefore, if a failure occurs over the V1, called decisional speed, the pilot must continue the take-off since there would be not enough runway left for breaking.

2.5.2 Landing analysis

The landing analysis is similar to the take-off one. This phase begins once the aircraft descends below a 50-foot obstacle and concludes with a full stop on the runway. According to *CS-25* [13] regulations, the landing distance obtained from the analysis must be multiplied by 1.666 to account for pilot performance and other conditions that may extend the landing distance. It is important to note that during the certification process, thrust reversers are not considered in determining the landing distance because an engine failure would render them inoperative. The following figure shows the various stages of landing phase, which will be detailed below.

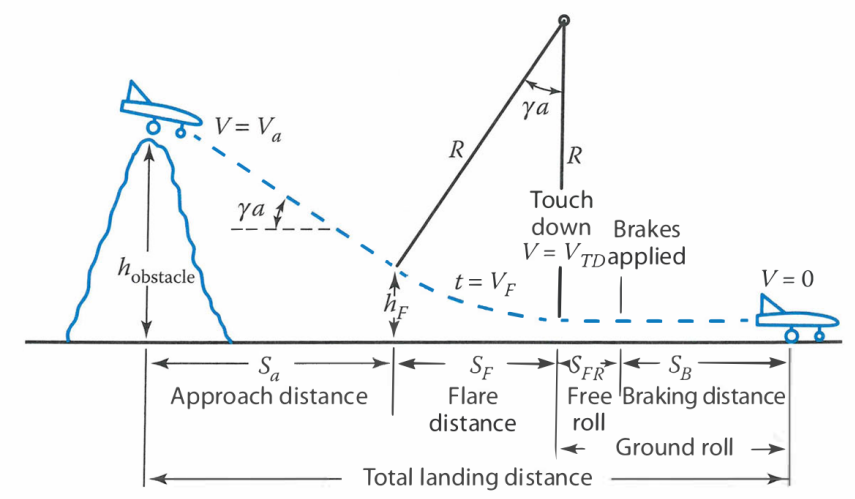

Figure 2.5: Landing phases division [12,13].

- *Approach*: the distance travelled during this phase, is defined as the one, projected on the ground, travelled by the aircraft descending from the obstacle height to the height at which the flare maneuver begins. This distance is evaluated as

$$S_A = \frac{h_{obstacle} - h_{TR}}{tan\,\gamma}$$

where the approach angle is γ, which must be no bigger than 3°. To ensure that, it must be verified that the aircraft has sufficient thrust to maintain this descent angle, with the approximation that

$$\frac{T}{W} = sin\,\gamma + \frac{1}{L/D}$$

The approach velocity is 1.3 times the stall velocity in landing configuration.

- *Flare*: this is considered a circular maneuver with radius

$$R = \frac{V_F^2}{g(n-1)}$$

The load factor n is estimated at 1.2, while the flare velocity is 1.23 times the stall speed in landing configuration. This particular speed value is indicated by the ICAO as *Approach Speed at Runway Threshold* and is used to categorize the aircraft based on their approach speed, in order to provide the necessary separation in landing paths.

- *Free roll*: This distance is added to the computation of the total landing distance to account for the delay between touch-down and the activation of the brakes. Since the speed can be considered constant and the delay ranges between 2 and 3 seconds, this distance is evaluated as $2.5 \cdot V_{touch-down}$; the touch-down speed is 1.15 times the stall speed in landing configuration. The thrust is considered fixed at the idle value, since no thrust reversers can be considered in this analysis.

The conclusions of this analysis establish in which airports the aircraft will be able to operate, depending on the runway length necessary to satisfy the CS-25 standards.

2.5.3 Performances verification

The aim of the conceptual design is to assess the feasibility of both the vehicle and the mission concept, considering technical and operational aspects, discussed in this section [10]. This requirements verification process imposes performance constraints on the aircraft design process, particularly concerning the aircraft weight, wing surface area and thrust. These requirements are expressed in terms of wing loading and thrust to weight ratio:

$$Wing\ loading = \frac{W}{S} \qquad Thrust\ to\ Weight\ ratio = \frac{T}{W}$$

While the thrust to weight ratio does not influence the calculations loop, the first one is a discriminant factor for the convergence of the method.

Each requirement defined below is linked to a specific mission phase: landing and instantaneous turn are involved the wing loading constraints, while take-off, cruise, climb, second segment and the sustained turn set the thrust-to-weight ratio lower limitations. Being all these phases related to different conditions (altitude, speed and atmospheric characteristics), all the figure of merits refer to the sea level conditions and to the Maximum Take-Off Weight.

Wing loading requirements

To identify the dimensioning value, the smallest wing loading will be selected (see Section 3) to not oversize the wing structural weight. In each of the following phases, a minimum value of wing loading is necessary.

LANDING

$$\frac{W}{S} = \frac{\rho V_{lnd}^2 C_{L_{lnd}}^2}{2g}$$

The parameters involved are listed below:

- $C_{L_{lnd}}$ is the lift coefficient in landing configuration, assumed as the maximum lift coefficient in the subsonic conditions. It comes from the aerodynamic database.
- V_{lnd} is the landing speed, as calculated during the landing analysis it is related to the landing distance.

- ρ is the air density at the airfield altitude.
- g is the acceleration of gravity.

For the landing requirement the reference weight is the MTOW because, in case of emergency, the aircraft shall be able to successfully land straight away.

INSTANTANEOUS TURN

$$\frac{W}{S} = \frac{\rho g R_{turn} C_{L_{turn}} \cdot \sqrt{n_{turn}^2 - 1}}{2 \cdot n_{turn} \cdot g}$$

For this analysis, the implemented equation is rewritten as follows, since the turn rate is a known parameter. In fact, according to the normative, the airplane must be able to reach an angle of 360° turn in two minutes, so the turn rate value must be equal to 3 deg/s.

$$\frac{W}{S} = \frac{\rho g R_{turn} C_{L_{turn}} \cdot V^2}{2 \cdot n_{turn} \cdot g} \sigma$$

Where:

- V is the speed; it is a user input though the Mach number and the altitude.
- ρ is the air density at the selected altitude.
- σ is the density ratio, defined as

$$\sigma = {\rho_{SL}}/{\rho}$$

  Being ρ the atmospheric density at the user-input altitude.

- $C_{L_{turn}}$ is the maximum lift coefficient in subsonic conditions. It comes from the aerodynamic database.
- n is the load factor, according to the equation

$$n = \sqrt{1 + \left(\frac{V\dot{\psi}}{g}\right)^2}$$

$$\dot{\psi} = 3\,{deg}/{s} = 0.05236\,{rad}/{s}$$

Thrust requirements

The take-off, climb, cruise and second segment phases determine the thrust-to-weight ratio requirements. In this context, the most stringent requirement is the highest one, as the aircraft must not be oversized. For this analysis the two cases subsonic and supersonic have been distinguished and the reference weight is not the MTOW but the one relative to each phase, as calculated in the previous fuel consumption estimation.

TAKE-OFF

For this phase the reference equation is

$$\frac{T}{W} = \frac{W/S}{\rho \cdot C_{L_{TO}} \cdot P}\sigma$$

In which the involved parameters are listed below:

- $\frac{W}{S}$ is the wing loading, with *MTOW* as reference weight for this phase.
- $C_{L_{TO}}$ is the take-off lift coefficient.
- P is a user-input parameter depending on the type of aircraft and the definition of take-off length [12], as shown in the graph below:

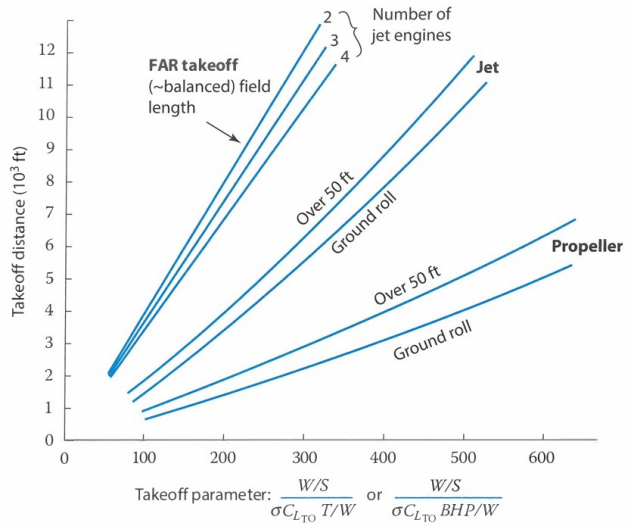

Figure 2.6: Take-Off parameter for Take-Off requirement thrust verification [12].

If considering the balanced field length, the distance is defined as the one travelled from the stopped aircraft at the beginning of the runway to the reaching of the decisional speed.

If considering the case of over 50 ft, the covered distance is considered from the stopped aircraft condition to the cleared obstacle condition.

If the definition used is ground roll, the length considered is the one covered to the complete detachment of the main undercarriage from the ground.

- σ is the density ratio, same definition as before.

The equation shows linear dependence between $\frac{W}{S}$ and $\frac{T}{W}$. The density ratio accounts the effect of the airport altitude: if the altitude increases, the air density decreases and so does σ, while, with the same value of wing surface, a lower level of lift is generated. This makes the $\frac{T}{W}$ ratio increase.

On the other hand, $\frac{T}{W}$ decreases if $C_{L_{TO}}$ increases, which leads to a lower necessary thrust at parity of wing loading, or a smaller wing surface keeping the engine fixed.

CLIMB

$$\frac{T}{W} = \frac{\frac{1}{2}\rho V_{climb}^2 C_{D_{climb}}}{\pi g \frac{W}{S}} + \frac{V_S}{V_{climb}}$$

During this phase, the stationary hypothesis cannot be done. On the other hand, it will be considered as a single segment from take-off to cruise for the subsonic case and from the subsonic cruise to the supersonic cruise for the supersonic case.

- V_{climb} is the climb speed, defined by user.
- V_S is the vertical speed. At this stage it may be defined by user, eventually being adjusted during the subsystems design (i.e. the Environmental Control System).
- C_D is the drag coefficient at the considered climb conditions. It will be derived from the aerodynamic database.
- ρ is the air density.

- $\frac{W}{S}$ is the wing loading. For this case the reference weight was set as

$$W = \frac{W_{final}}{W_i} \cdot MTOW$$

Being W_i the aircraft weight at the beginning of the phase and W_{final} the aircraft weight at the end. The same considerations are valid for the supersonic climb as well. These considerations are necessary due to non-stationary nature of this phase during which the fuel present onboard undergoes a large variation. However, this is still an approximation: the exact calculation would derive from the differentiation of the fuel variation with time low.

It is clear that, if the drag developed increases, higher levels of trust to weight ratio are needed.

CRUISE

$$\frac{T}{W} = \frac{\frac{1}{2}\rho V_{cruise}^2 C_D}{\pi g \frac{W}{S}} \sigma$$

The variables involved are:

- σ, same definition as before. For the subsonic cruise the air density considered is the one corresponding to that phase altitude, set by user. At the same way, for the supersonic cruise the density was calculated at the supersonic cruise altitude.
- V is the subsonic or supersonic cruise speed, derived from the Mach number and altitude defined by the user.
- C_D is the aerodynamic drag coefficient, derived from the aerodynamic database with the conditions of altitude and speed set by the user.
- $\frac{W}{S}$ is the wing loading. The considerations made for the climb phase are valid for subsonic and supersonic cruise phases too, so the reference weight is defined as

$$W = \frac{W_{cr,final}}{W_{cr,i}} \cdot MTOW$$

Distinguishing for the subsonic and the supersonic cruise. Here several parameters have impact:

- If the cruise speed increases $\frac{T}{W}$ increase or, keeping the engine fixed, a lower wing surface is necessary.
- If the aircraft design is such as to increase the drag coefficient, high performances are required to the propulsive system.
- If the cruise altitude increases, the air density decreases and so does $\frac{T}{W}$.
- The cruise can be performed with a lower level of thrust if the wing loading increases through the only wing surface (i.e. keeping W fixed).

SECOND SEGMENT

$$\frac{T}{W} = \frac{N_e}{N_e - 1}\left(\frac{C_D}{C_L} + G_{2nd}\right)$$

The second segment definition is a regulatory requirement. It describes the necessity, for the aircraft, to continue the climb with a minimum gradient even in one engine inoperative condition. It depends on:

- N_e is the number of necessary engines.
- C_D is the aerodynamic drag coefficient, determined from the aerodynamic database in the take-off conditions.
- C_L is the aerodynamic lift coefficient, determined from the aerodynamic database in the take-off conditions.
- G_{2nd} is the minimum climb gradient, set by user.

SUSTAINED TURN

Sustained turn is defined as a turn performed at constant altitude and speed defined by the user.

$$\frac{T}{W} = \frac{\frac{1}{2}\rho V_{cr}^2 C_{D_0}}{\frac{W}{S}g} + \frac{W}{S}g\frac{n_{turn}^2}{\frac{1}{2}\rho V_{cr}^2 \pi A e}$$

It depends on the following parameters:

- ρ is the atmospheric density at the considered altitude.
- V_{cr} is the cruise speed.
- C_{D_0} is the parasite drag, derived from the aerodynamic database at the established conditions.
- $\frac{W}{S}$ is the wing loading, with MTOW as reference weight.
- n_{turn} is the load factor.
- A is the reference wing surface.
- e is the Oswald factor.

2.5.4 Matching chart

The matching chart, introduced by NASA in 1980, is a graphical tool that represents power plant configurations in relation to their requirements [10]. In this graph, each of the previously calculated equations are displayed, so that each curve represents the corresponding phase requirements in term of necessary thrust and wing loading.

The principle is that the wing shall provide enough lift during all the phases of the mission, at the same time selecting the wing loading that minimizes the structural weight. For what regards the $\frac{T}{W}$, the engine should be able to generate sufficient thrust.

The *feasibility area* is the one determined by the most stringent requirements through the corresponding curves. Each point inside this area is a feasible aircraft concept, as it would satisfy all the requirements listed above. Regarding the wing loading, the optimum design points would be the ones determined by the possible minimum wing surface in order to not oversize the structure weight, ensuring at the same time the generation of the necessary lift

level. At the same time, the optimum thrust to weight ratio would be the lowest possible, according to the requirements in terms of performance necessary to the exploitation of the mission.

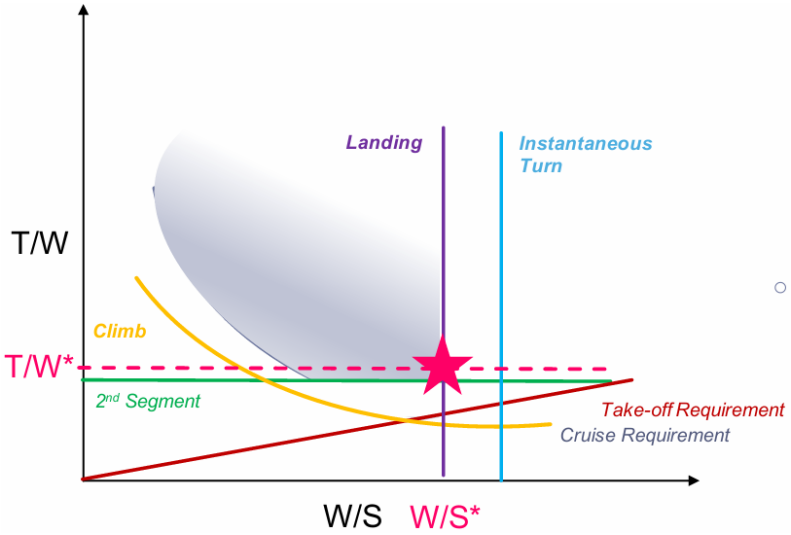

Figure 2.7: Matching chart example [10].

The one shown above is an example of a generic matching chart, with all the features discussed above. Since the case study expects both supersonic and subsonic phases, two matching charts were produced, considering the various contributions accordingly.

Subsonic case requirements:

- Landing
- Instantaneous turn
- Take-off run
- Subsonic climb
- Subsonic cruise
- Sustained turn
- Second segment

Supersonic case requirements:

- Supersonic climb
- Supersonic cruise

For the supersonic phases, all the other requirements are not involved because the phases at which those requirements refer are not included in the supersonic phases of the mission. Furthermore, the wing loading requirements are more restrictive if computed whit reference to the subsonic regime, where the atmospheric density is higher due to the lower altitude.

At this point, the user should be able to estimate the feasibility of the project visualizing the design point resulting from the conceptual design inside the matching chart.

SECTION 3

Case study and algorithm implementation

In this section, the theories and approaches discussed are applied to an example case study. All the chapters above will be faced from a practical point of view, thus explaining how the tool developed in MATLAB environment works.

In the figure above, the green and the red dots are, respectively, the start and the end of the algorithm. The light-blue boxes represent a section of the tool, each one described by one of the next paragraphs. The green boxes stand for the main MATLAB functions “called” in the script *main.mat*, while the white ones are called by one, or more, of the green others. In fact, the function *main.mat* has the only scope of running the other ones, where the real analysis and calculations are performed. The overall process will be discussed in detail.

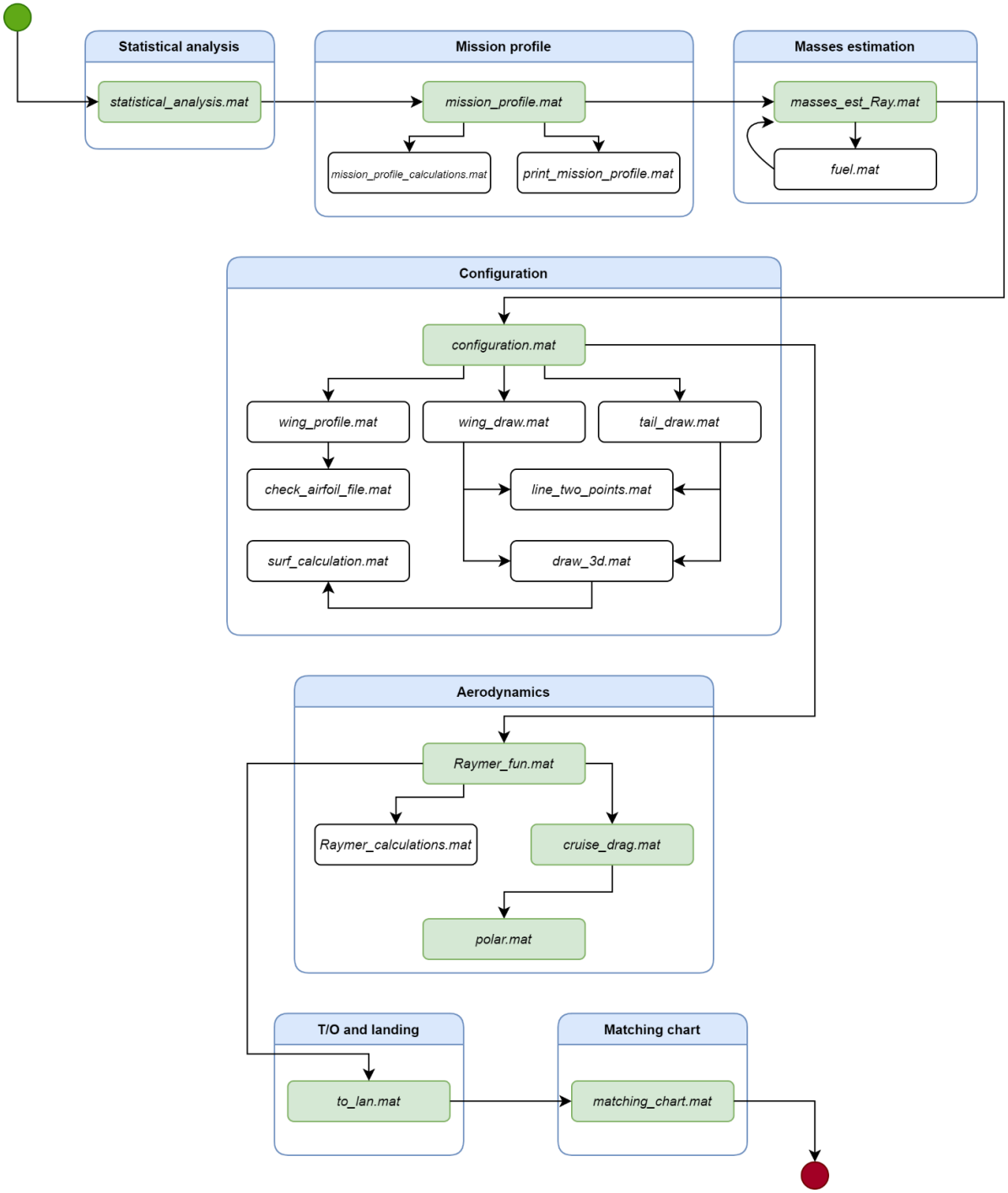

Figure 3.1: Algorithm overall flow.

3.1 Statistical analysis

The starting point of any statistical analysis is the creation of a database, in this case, made of reference aircraft. The understanding of the existing technologies is fundamental to make a prevision of where the new project will take place, and it constitutes the basis to evaluate the feasibility of a new conceptual design.

The reference aircraft database is composed of projects which eventually saw the operative phase and others which remained at the conceptual stage of the process. This and the fact that they are, in general, quite dated, poses the basis to reflect on the reliability of the results based on such an analysis. As a matter of fact, those results must be considered *only* as the input data for the subsequent design loops.

The selection of the database has been conducted based on the high-level mission requirements, which have already been briefly summarized in Table 1.1. For what concerns the propulsive system there are no examples in literature, so the aircraft have been selected among those propelled with kerosene.

3.1.1 Reference aircraft

For each one of the aircraft considered, the most significant parameters have been evaluated:

- Payload
- MTOW
- Cruise Mach
- Range
- Thrust
- Wing surface
- Wingspan
- Length
- Propellant mass
- Propellant mass fraction (PMF)

SUKHOI T-4

The Sukhoi T-4 [14] was a Soviet supersonic strategic bomber prototype developed during the 1960. Nicknamed "Sotka", it was designed to perform high-speed, high-altitude missions, primarily targeting U.S. naval groups. Capable of reaching speeds up to Mach 3, the T-4 was a competitor to the American SR-71 Blackbird and XB-70 Valkyrie. The T-4 featured a variable geometry nose, unique titanium and steel construction to withstand the extreme temperatures at supersonic speeds, along with advanced avionics for its time. Despite promising test flights, only a few prototypes were built due to high costs and technical challenges.

Specifications	
Passengers	2
MTOW [kg]	110000
Propellant weight [kg]	35000
PMF	0.32
Cruise Mach	3
Range [km]	6000
Thrust [kN]	640
Wing surface [m^2]	296
Wingspan [m]	22
Length [m]	44.5

Table 3.1: Sukhoi T-4 specifications [14].

Figure 3.2: Sukhoi T-4 [14].

TUPOLEV Tu-444

The Tupolev Tu-444 [15] was a proposed supersonic business jet concept developed by the Russian aerospace company Tupolev in the early 2000s. It was intended to serve the growing demand for faster intercontinental business travel. Designed to fly at speeds of Mach 2, the Tu-444 would have drastically reduced travel times compared to traditional business jets. It was envisioned to carry around 6 to 10 passengers over distances of up to 7000 km. However, due to technical challenges, high development costs, and a lack of market demand, the Tu-444 never progressed beyond the conceptual phase.

Specifications	
Passengers	10
MTOW [kg]	41000
Propellant weight [kg]	20300
PMF	0.50
Cruise Mach	2.2
Range [km]	7500
Thrust [kN]	190
Wing surface [m^2]	136
Wingspan [m]	16
Length [m]	36

Table 3.2: Tupolev TU-444 specifications [15].

AERION SBJ

The Aerion SBJ (Supersonic Business Jet) [16] was a proposed supersonic business jet developed by the American company Aerion Corporation. Designed in the early 2000s, the SBJ aimed to be the first private jet capable of flying at speeds up to Mach 1.6. The jet was planned to carry 8 to 12 passengers over distances of around 7400 km. One of the key innovations was its "natural laminar flow" wing design, which would have reduced drag and fuel consumption, making the aircraft more efficient. The SBJ also aimed to address noise concerns by minimizing sonic booms during overland flights.

Specifications	
Passengers	12
MTOW [kg]	40820
Propellant weight [kg]	20900
PMF	0.51
Cruise Mach	1.8
Range [km]	7800
Thrust [kN]	174
Wing surface [m^2]	101
Wingspan [m]	19.6
Length [m]	45.2

Table 3.3: Aerion SBJ specifications [16].

Figure 3.3: Aerion SBJ [16].

QSST

The QSST (Quiet Supersonic Transport) [17] was a supersonic aircraft concept developed by SAI (Supersonic Aerospace International) in collaboration with Lockheed Martin in the early 2000s. The goal of the QSST was to create a business jet capable of supersonic flight while minimizing the disruptive sonic boom typically associated with such speeds. It was designed to fly at Mach 1.8 and carry around 10 to 12 passengers over distances of up to 7400 km.

Despite the ambitious vision, the QSST development never progressed beyond the conceptual stage. The project remains a significant attempt to comply with overland flight regulations.

Specifications	
Passengers	20
MTOW [kg]	11020
Propellant weight [kg]	4708
PMF	0.43
Cruise Mach	1.7
Range [km]	7400
Thrust [kN]	294
Wing surface [m^2]	186
Wingspan [m]	19.2
Length [m]	40.3

Table 3.4: QSST specifications [17].

Figure 3.4: QSST [18].

SPIKE S-512

The Spike S-512 [19] is a supersonic business jet concept developed by Spike Aerospace, aimed at revolutionizing private air travel. Designed to fly at speeds of up to Mach 1.6, the S-512 promises to significantly reduce travel times for long-haul flights. It is intended to accommodate around 12 passengers in a spacious, luxurious cabin. One of the key features of the S-512 is its innovative design, which incorporates a “quiet supersonic” technology to minimize the sonic boom effect, allowing overland supersonic flight. The aircraft is also designed to have advanced aerodynamics and lightweight materials to improve fuel efficiency.

Specifications	
Passengers	18
MTOW [kg]	52160
Propellant weight [kg]	25400
PMF	0.49
Cruise Mach	2.8
Range [km]	11500
Thrust [kN]	178
Wing surface [m^2]	164
Wingspan [m]	18
Length [m]	37

Table 3.5: Spike S-512 specifications [19].

AERION AS2

The Aerion AS2 [16,20] is a supersonic business jet designed by Aerion Corporation, aiming to combine speed, luxury, and efficiency in private air travel. Capable of flying at speeds up to Mach 1.4, the AS2 is intended to significantly reduce flight times for long-distance journeys, making it a desirable option for business travelers.

Specifications	
Passengers	11
MTOW [kg]	68040
Propellant weight [kg]	32000
PMF	0.47
Cruise Mach	1.4
Range [km]	7800
Thrust [kN]	240
Wing surface [m^2]	140
Wingspan [m]	24
Length [m]	44.2

Table 3.6: Aerion AS2 specifications [16].

Figure 3.5: Aerion AS2 [20].

BOOM OVERTURE

The Boom Overture [21,22] is a next-generation supersonic airliner under development by Boom Supersonic, aiming to bring back commercial supersonic flight, last seen with the retirement of the Concorde in 2003. Designed to fly at Mach 1.7 (approximately 2100 km/h), the Overture will more than double the speed of current commercial aircraft. It will accommodate 65-80 passengers and significantly reduce flight times, with transatlantic routes like New York to London expected to take under 4 hours. The aircraft will have a range of 7870 km, making it ideal for long-haul international routes. A key goal of the project is sustainability: the Overture will be powered by sustainable aviation fuels (SAF) to operate carbon-neutral flights, addressing the environmental concerns that previously plagued both supersonic and subsonic aviation.

Boom has already built a prototype called XB-1, which serves as a technological demonstrator for the Overture. The first test flight of the Overture is scheduled for 2027, with entry into commercial service by 2029. Some of the major airlines have already placed pre-orders, signaling strong interest in this faster and more sustainable way of travelling.

Specifications	
Passengers	72
MTOW [kg]	77111
Propellant weight [kg]	38600
PMF	0.50
Cruise Mach	1.7
Range [km]	7870
Thrust [kN]	356
Wing surface [m^2]	218
Wingspan [m]	32.3
Length [m]	61.2

Table 3.7: Boom Overture specifications [21].

Figure 3.6: Boom Overture [21].

CONCORDE

The Concorde [23] was a British-French turbojet-powered supersonic passenger airliner that revolutionized air travel. Developed jointly by British Aircraft Corporation and Aérospatiale, it first flew in 1969 and began commercial service in 1976. Capable of flying at speeds up to Mach 2.04, the Concorde drastically reduced flight times on transatlantic routes, such as New York to London, which could be completed in approximately 3.5 hours. The aircraft featured a distinctive delta wing design and variable shape, with a capacity of about 100 passengers, the Concorde offered a luxurious travel experience.

Despite its technological advancements and iconic status, the Concorde faced challenges, including high operational costs, noise restrictions due to its sonic boom, and increasing

competition from subsonic jets. Following the tragic crash of Air France Flight 4590 in 2000 and a decline in passenger numbers, the Concorde was retired in 2003. It remains an iconic symbol of innovation and luxury travel.

Specifications	
Passengers	110
MTOW [kg]	185066
Propellant weight [kg]	97600
PMF	0.53
Cruise Mach	2
Range [km]	6230
Thrust [kN]	676
Wing surface [m^2]	358
Wingspan [m]	25.5
Length [m]	62.1

Table 3.8: Concorde specifications [23].

Figure 3.7: Concorde [23].

TUPOLEV TU-144

The Tupolev Tu-144 [24], often referred to as the "Concordski" (for its similarity to the Concorde), was a Soviet supersonic passenger airliner, notable for being one of the first commercial supersonic aircraft to enter service. It made its first flight in 1968. The Tu-144 was designed to operate on long-haul routes and could reach speeds of up to Mach 2.15. Featuring a distinctive canard wing configuration and four engines, it could carry around 140 passengers in a configuration similar to that of the Concorde. The aircraft was eventually retired in 1983 due to high operating costs and increasing competition from subsonic jets.

Specifications	
Passengers	150
MTOW [kg]	205000
Propellant weight [kg]	95000
PMF	0.46
Cruise Mach	2.17
Range [km]	6500
Thrust [kN]	980
Wing surface [m^2]	507
Wingspan [m]	28.8
Length [m]	65.7

Table 3.9: Tupolev TU-144 specifications [24].

Figure 3.8: Tupolev TU-144 [24].

BOEING 2707

The Boeing 2707 [25] was a proposed supersonic transport (*SST*) aircraft designed by Boeing in the 1960s. It aimed to compete with the Concorde and the Soviet Tupolev Tu-144, promising to carry passengers at speeds of up to Mach 2.7. The 2707 was designed to accommodate approximately 250 to 300 passengers, making it significantly larger than its competitors. One of the most innovative features of the 2707 was its variable-geometry wings, which could be adjusted for optimal performance during takeoff, cruising, and landing. This design was intended to enhance aerodynamic efficiency and reduce drag at supersonic speeds. Despite its ambitious design and potential, it never achieved the operative stage and the project was ultimately canceled in 1971.

Specifications	
Passengers	218
MTOW [kg]	340000
Propellant weight [kg]	166500
PMF	0.49
Cruise Mach	2.7
Range [km]	6685
Thrust [kN]	1160
Wing surface [m^2]	865
Wingspan [m]	43.72
Length [m]	91.44

Table 3.10: Boeing 2707 specifications [25].

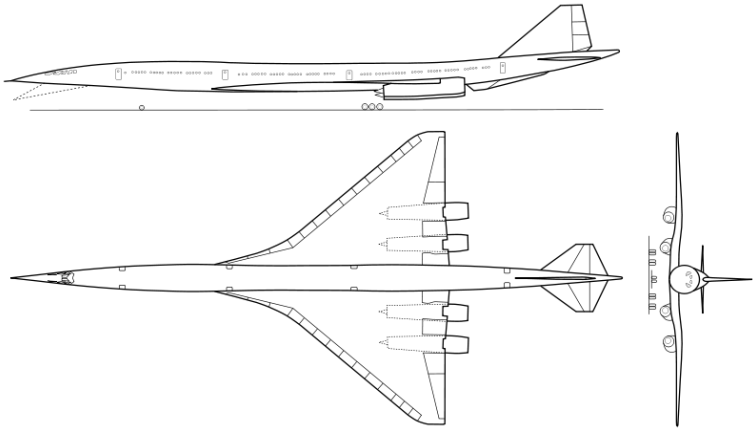

Figure 3.9: Boeing 2707 [25].

XB-70 VALKYRIE

The North American XB-70 Valkyrie [26] was an experimental supersonic bomber developed by North American Aviation in the 1960s. Designed to fly at speeds of up to Mach 3 and at altitudes of 70000 ft, the XB-70 aimed to penetrate enemy defenses at unprecedented speeds and altitudes, making it a key component of the U.S. Air Force's strategic capabilities during the Cold War. The aircraft featured a distinctive design with a large delta wing, which contributed to its aerodynamic efficiency at high speeds. It was powered by six GE YJ93 engines and had a unique configuration that included variable geometry wings, allowing for optimal performance during different phases of flight.

Only two prototypes of the XB-70 were built, with the first flight occurring in 1964. Despite its impressive performance capabilities, the program was eventually canceled in 1969.

Specifications	
Passengers	2
MTOW [kg]	27273
Propellant weight [kg]	140000
PMF	0.58
Cruise Mach	3.1
Range [km]	6900
Thrust [kN]	760
Wing surface [m^2]	585
Wingspan [m]	32
Length [m]	56.6

Table 3.11: XB-70 Valkyrie specifications [26].

Figure 3.10: XB-70 Valkyrie [26].

LOCKHEED L-2000

The Lockheed L-2000 [27,28] was a proposed supersonic passenger airliner concept developed by Lockheed Corporation in the 1960s, designed to compete with the British-French Concorde and the Soviet Tu-144 in the supersonic transport market. The L-2000 was envisioned to operate at speeds of up to Mach 3 and to carry around 250 passengers on transcontinental routes. One of the key features of the L-2000 was its innovative design, which included a delta wing configuration and variable geometry wings for optimal performance during various phases of flight.

Specifications	
Passengers	250
MTOW [kg]	267000
Propellant weight [kg]	150000
PMF	0.56
Cruise Mach	2.7
Range [km]	7870
Thrust [kN]	1160
Wing surface [m^2]	875
Wingspan [m]	35
Length [m]	83.26

Table 3.12: Lockheed L-2000 specifications [27].

Figure 3.11: Lockheed L-2000 [27].

TUPOLEV TU-244

The Tupolev Tu-244 [29] was a conceptual supersonic passenger airliner proposed by Tupolev, intended to be a successor to the Tupolev Tu-144. The Tu-244 was intended to fly at speeds of up to Mach 2.5 and was designed to carry around 250 passengers. While the Tu-144 nose could be tilted down for landing, in the Tu-244 concept the visual was provided to the pilots through cameras.

Specifications	
Passengers	266
MTOW [kg]	350000
Propellant weight [kg]	178000
PMF	0.51
Cruise Mach	2.5
Range [km]	9200
Thrust [kN]	980
Wing surface [m^2]	1200
Wingspan [m]	54.77
Length [m]	65.7

Table 3.13: Tupolev Tu-244 specifications [29].

3.1.2 Case study

For this and all the other charts in this work thesis, the following shapes and colors code is valid:

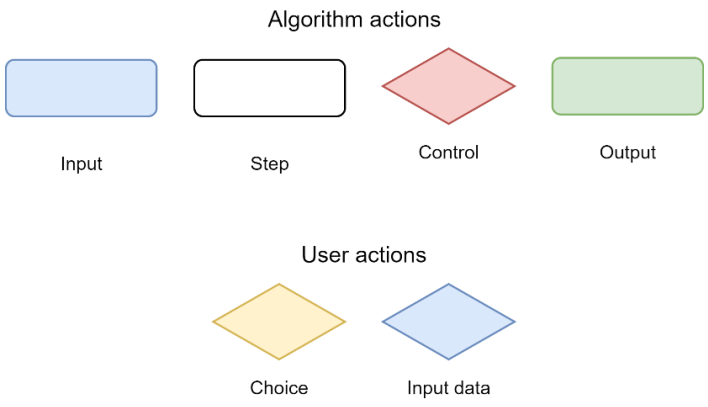

Figure 3.12: Algorithm legend.

Once defined the reference aircraft database, this is the input to the statistical analysis. The implemented process is shown in the flow chart below.

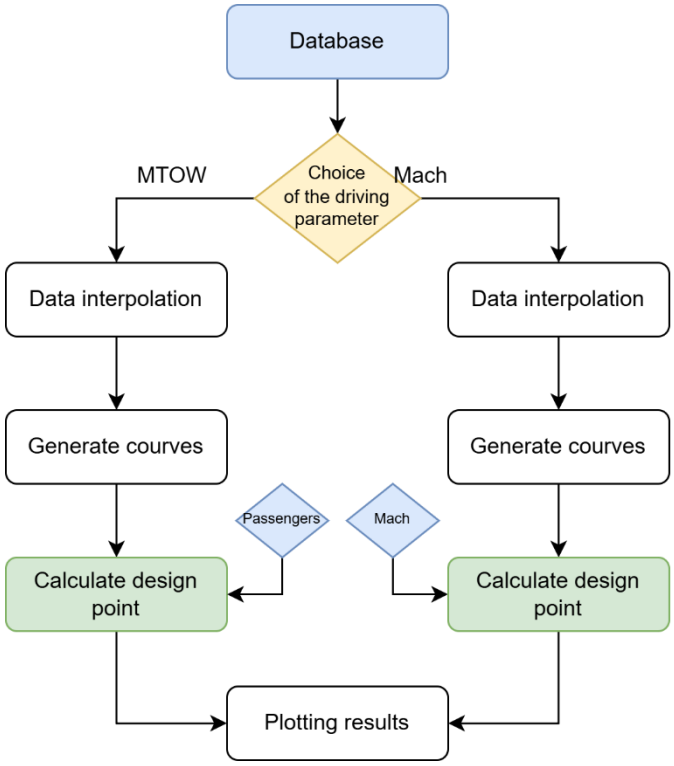

Figure 3.13: Statistical analysis flow chart.

As discussed before, the user must decide on one of the two possible driving parameters: MTOW, cruise Mach or all of them (not shown in the diagram). This can be done because choosing a variable rather than another as driver for the analysis has the effect of obtaining results which optimize that variable. Whatever the driver chosen by the user is, all data from database are interpolated in its function and the equation is created for each remarkable relation. At this point, looking at the zoom below, the algorithm performs this process in a loop in which every iteration the value of the variable of interest is increased:

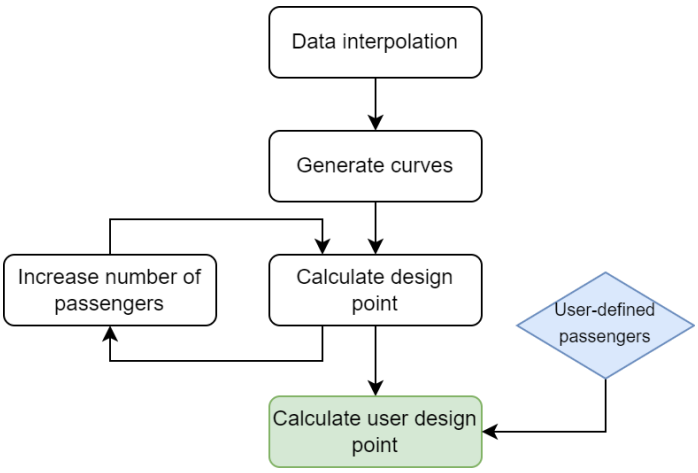

Figure 3.14: Statistical analysis flow chart (MTOW).

For the case of the MTOW the reference MATLAB function is *statistical_analysis_MTOW.mat;* since it is not part of the high-level requirements, the variable of interest is the passenger's number that, multiplied for the estimated weight of each one (120 kg), results in the payload weight. Being the required passenger for this case study equal to 70, this number ah been varied between 60 and 100. Every iteration a new design point is calculated and memorized and, at the end of the loop, all variables from this new "design points database" are interpolated in function of the passenger's number. Eventually, the user defined number is used as input for those equations to generate the definitive design point of the statistical analysis.

If, on the other hand, the set variable is the Mach number, that is the variable increased at each iteration, from 2.5 to 3.5, within the MATLAB function *statistical_analysis_mach.mat*. The minimum and maximum values have been chosen "around" the requirements, thus the user can be do a sort of off-design analysis even with the design point from statistical analysis only. For the purposes of this thesis the first option was selected and here are shown the graph results.

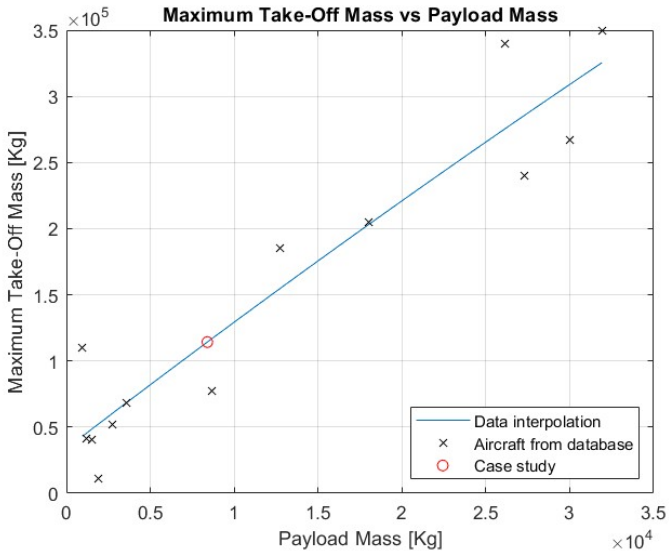

Figure 3.15: MTOW – Payload data interpolation.

The first interpolation is necessary to set, starting from the passenger's number entered by the user, the first-guess MTOW. It was found that a second-degree equation would have improved the reference data fitting. As expected, the trend is for the Maximum Take-Off Weight to increase with the payload weight.

The cruise Mach as a function of the MTOW shows an increasing quadratic trend, as shown in the next image. It may seem that with heavier aircraft the cruise speed stops increasing: the explanation could be that when the weight increases the geometrical dimensions generally do the same and so does the generated drug.

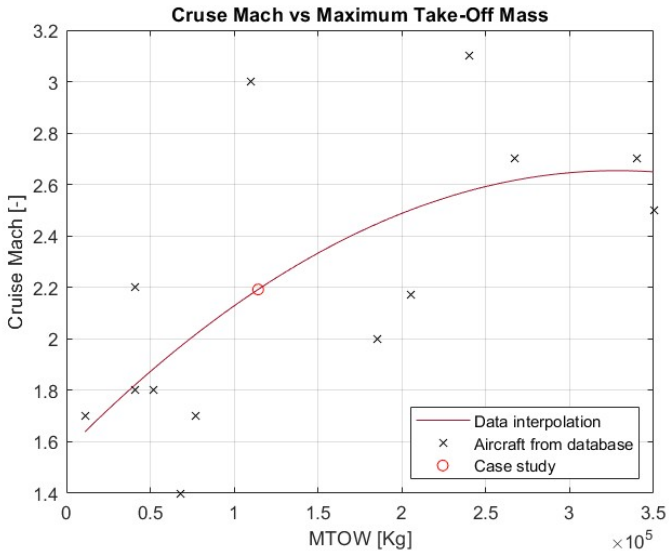

Figure 3.16: Mach - MTOW data interpolation.

In the next graph is shown the relation between the MTOW (which has been just set) and the Propellant Mass Fraction (PMF), defined as the ratio between the propellant weight and the MTOW. As in the previous case, the fitting was quadratic to maximize the square indetermination factor R^2. The propellant weight was calculated afterwards using the PMF, as

$$W_{fuel} = PMF \cdot WMTO$$

The fuel weight from database was not used due to uncertainty of data for some conceptual studies. According to the graph, there is one aircraft from database that appears to badly influence the trend: the Sukhoi T-4. Being a supersonic bomber, it is characterized by a high MTOW due to the presence of ballistic loads and only two crew members, and a low fuel weight, resulting in a low PMF. As a first trial it was removed from the database, but it was seen that this would have generally worsened the fidelity of the other analysis. Moreover, its absence in this specific case is not benefic as expected.

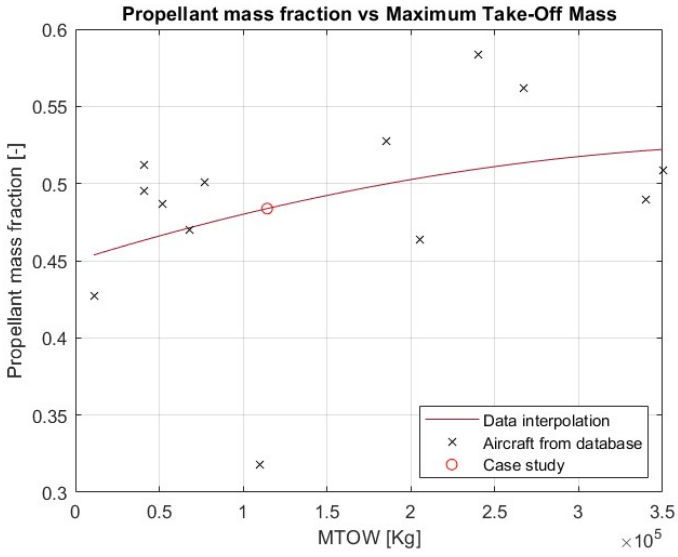

Figure 3.17: PMF - MTOW data interpolation.

The increase in the MTOW is also related to a larger wing surface because, maintaining the Mach number fixed, the necessary lift to be generated is higher. That's what resulted also in the analysis, as reported in the next figure, where the relation found between these two variables is quadratic. In this case it could be useful to see how the results would change performing the statistical analysis using the Mach number as driver parameter.

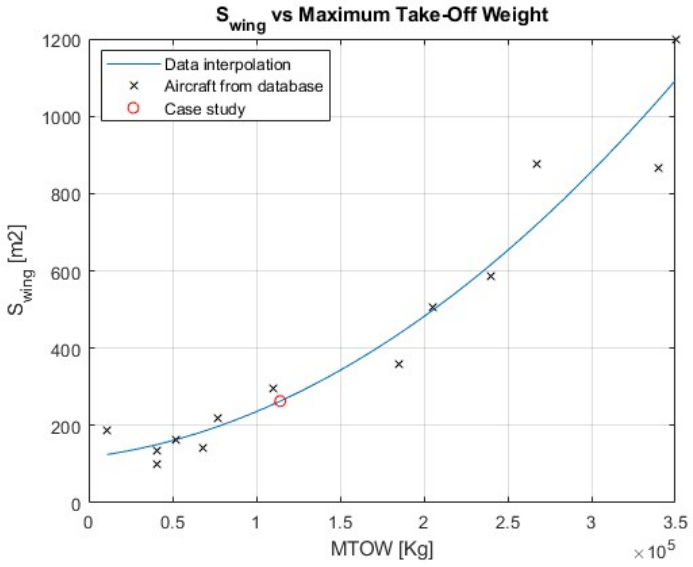

Figure 3.18: Wing surface - MTOW data interpolation.

The wingspan also is affected by the aircraft's weight, but with a linear relation as for the aircraft length. Regarding the last one, the increase is not caused by the higher weight but by the fact that, statistically, an aircraft heavier transports a larger number of passengers.

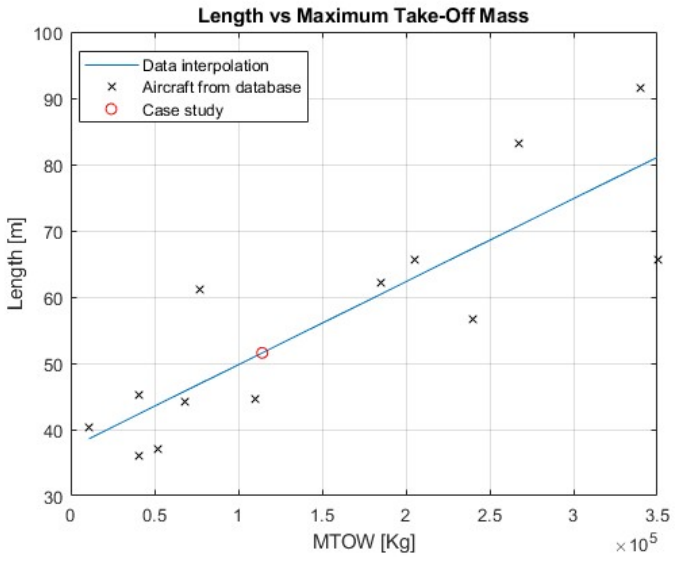

Figure 3.19: Length - MTOW data interpolation.

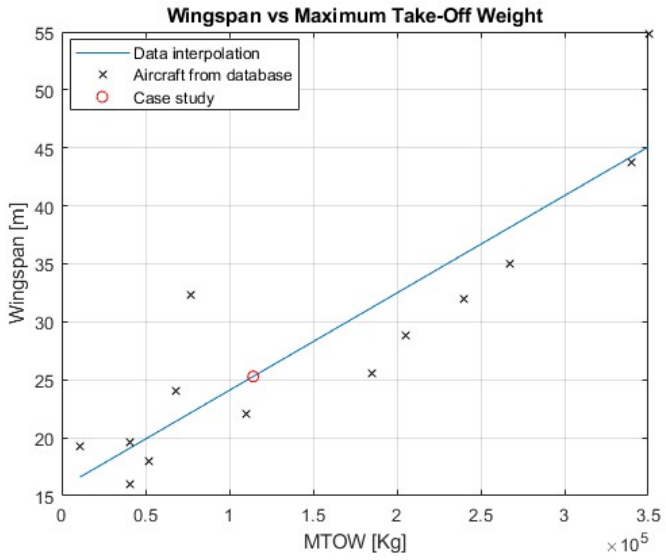

Figure 3.20: Wingspan - MTOW data interpolation.

More challenging to analyze is the case of the thrust. A first attempt was to calculate it, as done for the others, as function of the MTOW and of the Mach number. On the other hand, the results were not satisfactory, so the final approach was to calculate the latter as a function of the first MTOW only. The difference in the obtained thrust is sensitive, as reported in the first of the following figures, where the case study is the one obtained with the second approach.

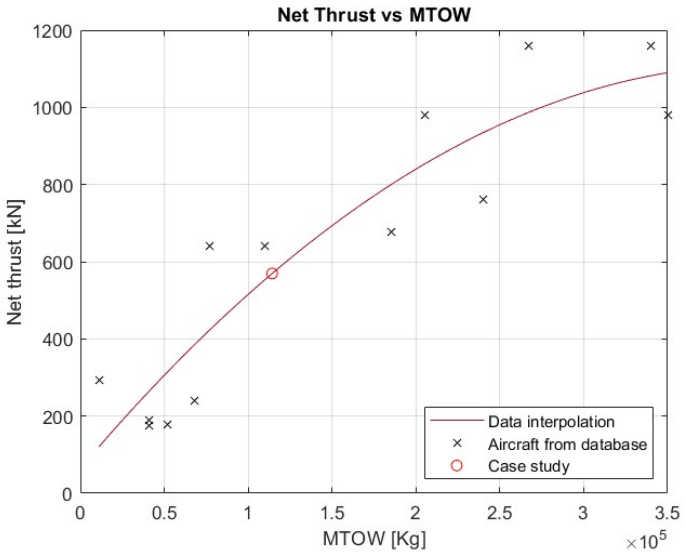

Figure 3.21 - Thrust - MTOW data interpolation.

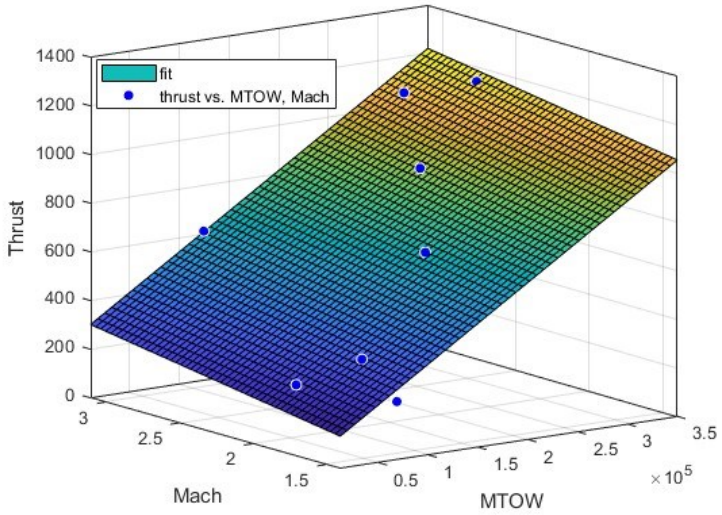

Figure 3.22: Thrust - Mach - MTOW data interpolation.

Finally, at the end of the analysis the results are shown to the user, as reported in the next figure, which represents a screenshot of the MATLAB command window.

```
================================================================================================
|-------------------------------- STATISTICAL ANALYSIS -------------------------------|
================================================================================================

Press:

    1 => Perform the statistical analysis with MTOW as driver
    2 => Perform the statistical analysis with Mach as driver
    3 => Perform the statistical analysis with all as drivers

Your choice is: 1
Set the number of passengers: 70

-------------------------------------------------
    First estimation from statistical analysis
-------------------------------------------------
Passengers          = 70
Maximum T/O Weight  = 114270.45 kg
Fuel mass           = 84493.96 kg
Payload mass        = 8400.00 kg
Empty weight        = 71229.49 kg
Cruise Mach         = 2.19
Wing surface        = 263.05 m2
Wingspan            = 25.29 m
Length              = 51.57 m
PMF                 = 0.48
Thrust              = 569.43 kN
```

Figure 3.23: Statistical analysis results (MTOW).

As it can be seen, this statistical analysis results in a lower cruise Mach as, according to the database, the “ideal” Mach number would be 2.19. Obviously, the further calculations have been done with Mach = 3.

As example, the results obtained choosing the Mach number as driver parameter are reported, being the implemented logic completely analogous to the previous case:

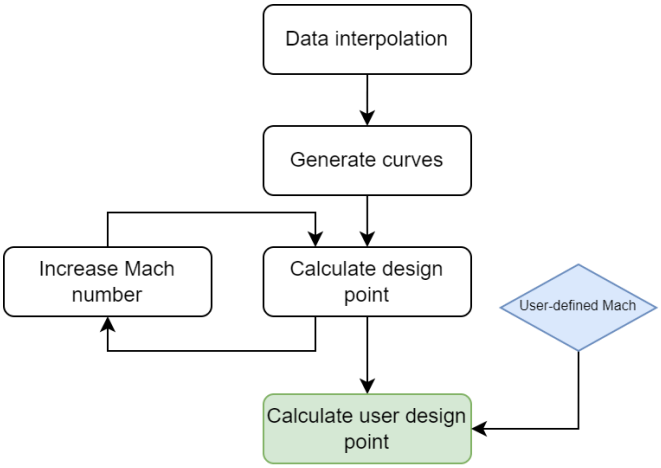

Figure 3.24: Statistical analysis flow chart (Mach).

Now the Mach number is set by the user and, for the same reasons detailed above, a database of possible design points is calculated increasing the Mach from 2.5 to 3.5. For the case of $M = 3$ the output interpolations are less accurate than the previous analysis due to the data from the aircraft database being quite scattered, but the trends obtained are interesting. Even in this case the bombers have the effect of “polluting” the database and the conceptual studies don’t provide reliable data.

The first diagram reported shows the Maximum Take-Off Weight as a function of the Mach number. As it could be expected, the aircraft with a higher cruise Mach are generally heavier, due to the larger fuel weight necessary to exploit the mission.

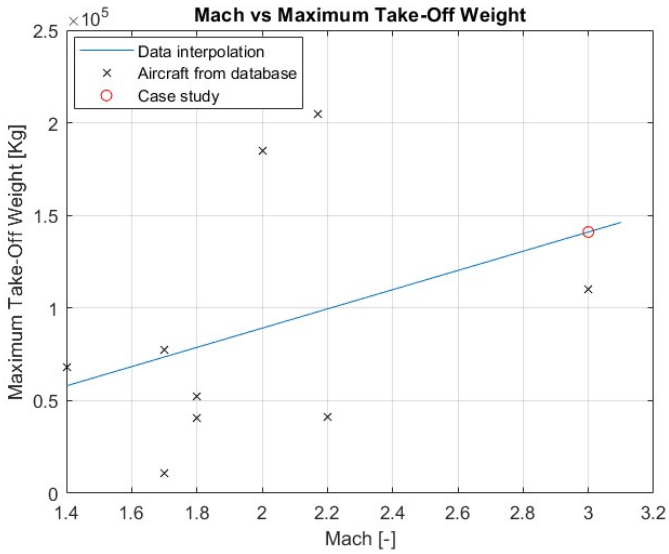

Figure 3.25: Mach - MTOW data interpolation.

For the Propellant Mass Fraction (PMF) the tendency is opposite, as aircraft designed for a higher Mach number tend to have a lower PMF. However, this does not necessarily lead to a lower amount of propellant needed for the mission. The reasons may lie in the different design features, in the fact that increasing the cruise Mach the aircraft are generally designed to be lighter, the higher cruise altitude that results in a lower level of drug generation, or a mix of those.

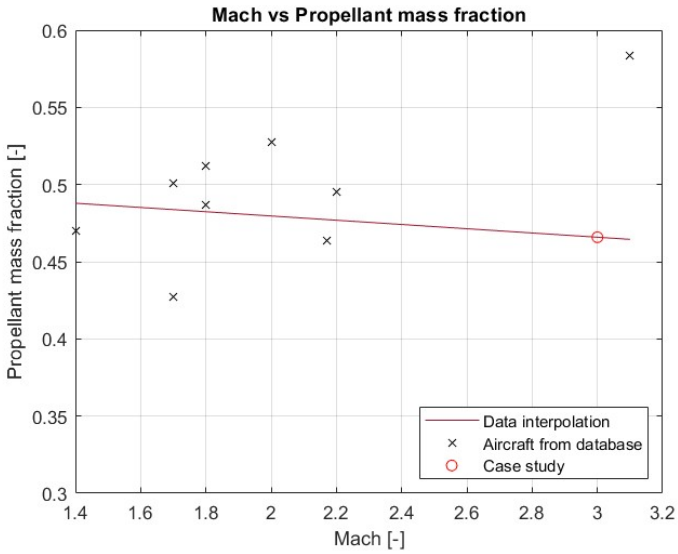

Figure 3.26: Mach - PMF data interpolation.

The fact that aircraft flying faster are generally lighter is also reflected in the number of passengers, that shows a decreasing trend.

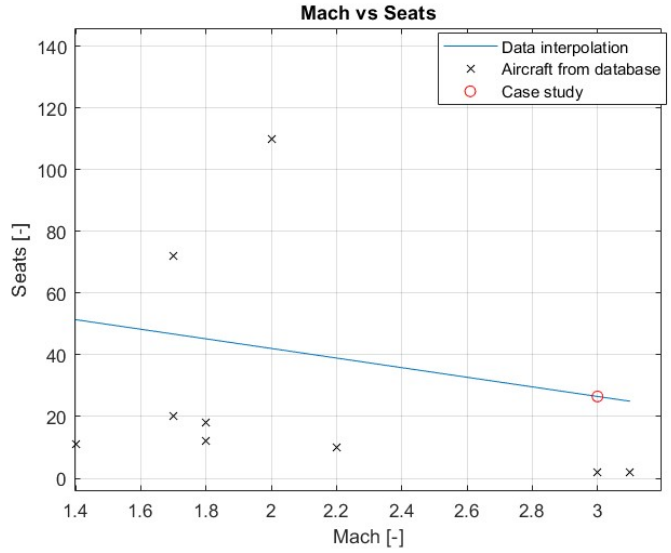

Figure 3.27: Mach - Seats data interpolation.

Conversely, the wing surface increases with the cruise Mach. This trend may be the result of several factors: maintaining fixed the other parameters, with a higher speed a smaller wing surface is needed to generate the necessary lift, but airplanes designed to fly faster usually have a higher cruise altitude, which means that the air density is lower and so it is the lift generated. Moreover, some aircraft in the database were designed to carry a large number of passengers, like the Tupolev Tu-244 (over 260 seats) and the Lockheed L-2000 (over 250 seats).

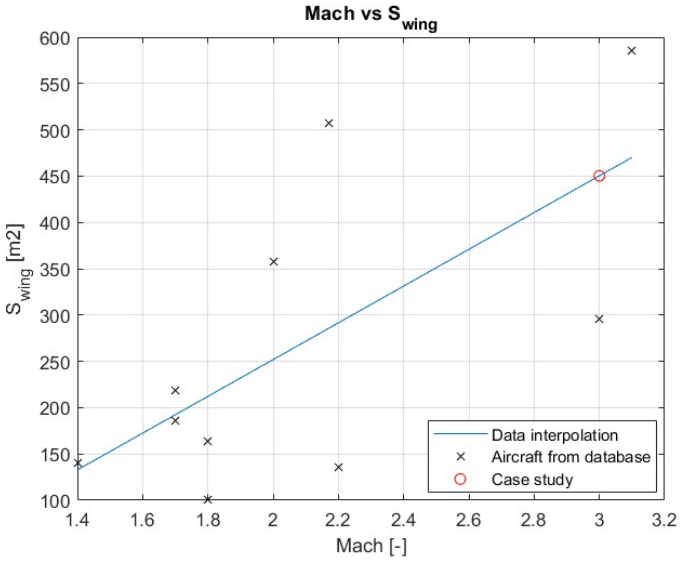

Figure 3.28: Mach - Wing surface data interpolation.

The other two geometric dimensions, wingspan and length, are characterized by an almost constant trend, as they are not directly related to the cruise Mach. There is a light increase in the wingspan, related to the increase in the wing surface, and in the aircraft length.

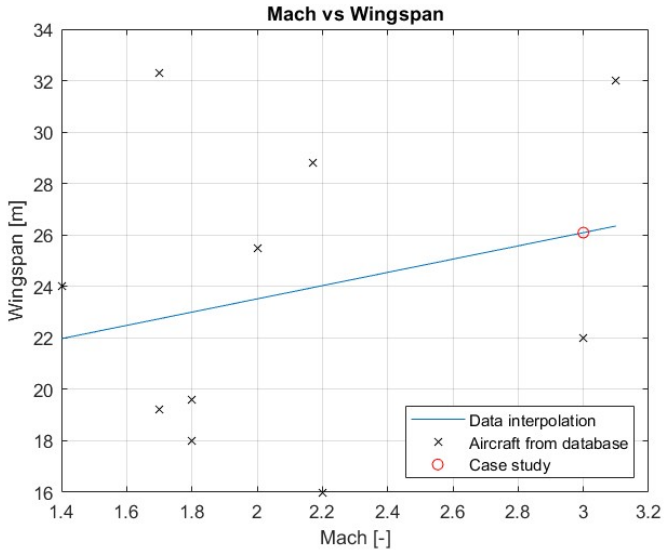

Figure 3.29: Mach - Wingspan data interpolation.

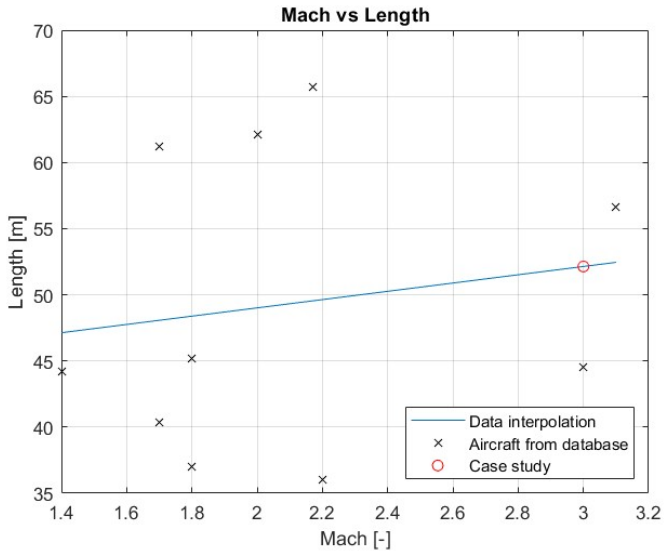

Figure 3.30: Mach - Length data interpolation.

For what concerns the thrust, the consideration made for the previous analysis remains valid, resulting in the following graphs:

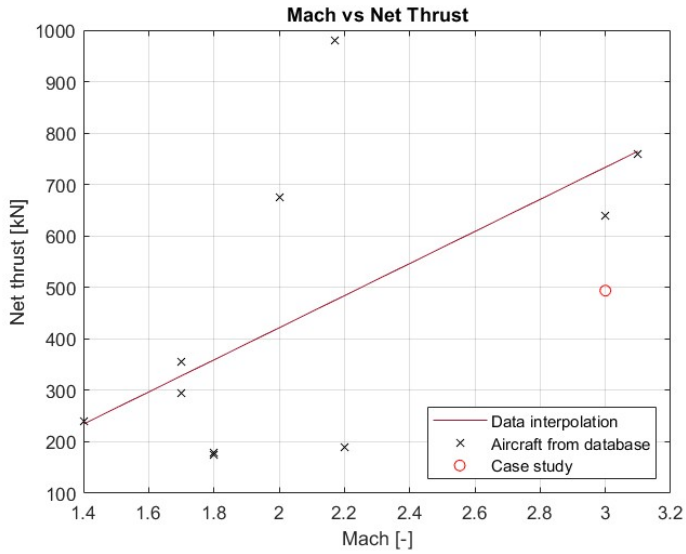

Figure 3.31: Mach - Thrust data interpolation.

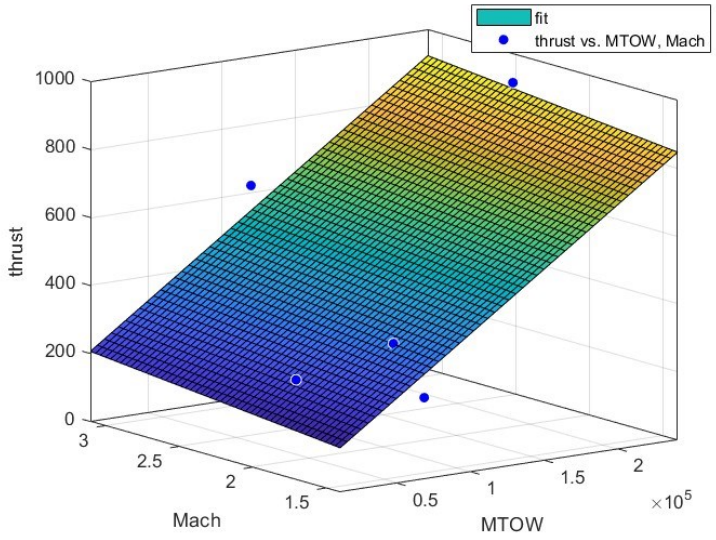

Figure 3.32: Mach - Thrust - MTOW data interpolation.

Once again at the end of the analysis a report is shown to the user.

```
================================================================================================
|------------------------------- STATISTICAL ANALYSIS -------------------------------|
================================================================================================

Press:

    1 => Perform the statistical analysis with MTOW as driver
    2 => Perform the statistical analysis with Mach as driver
    3 => Perform the statistical analysis with all as drivers

Your choice is: 2
Set the Mach number: 3

First estimation from statistical analysis:

Passengers          = 27
Maximum T/O Weight  = 141050.49 kg
Fuel mass           = 65710.57 kg
Payload mass        = 3180.03 kg
Empty weight        = 80124.45 kg
Wing surface        = 450.34 m2
Wingspan            = 26.09 m
Length              = 52.14 m
PMF                 = 0.47
Thrust              = 493.80 kN
```

Figure 3.33: Statistical analysis results (Mach).

In the previous case the user set the passengers number and it resulted in a different Mach number if compared to the mission requirement; now the second one is fixed and this led to a passenger number of only 27 which, according to the database, appears to be the “ideal” value. The other parameters are similar between the two analyses. In general, the user could obtain better results performing both and assigning opportune weight to the obtaining results. However, in this case, it was chosen to use the results obtained with the first one only, as 27 passengers is too far from the requisite.

In the next tables all the inputs and outputs of the statistical analysis are summarized.

Inputs	
Seats	70
Weight per seat [kg]	120
Cruise Mach	3
Cruise altitude [m]	18000
Range [km]	6000
Cruise air temperature [K]	216.65
Cruise air pressure [Pa]	7.5048e3
Cruise air density [kg/m^3]	0.1207
Cruise speed of sound [m/s]	295.0696

Table 3.14: Statistical analysis inputs

Outputs	
MTOW [kg]	114270
Fuel weight [kg]	84494
Payload weight [kg]	8400
Empty weight [kg]	71229
PMF	0.48
Wing surface [m^2]	263.05
Wingspan [m]	25.29
Length [m]	51.57
Thrust [kN]	569.43

Table 3.15: Statistical analysis outputs

3.2 Mission profile definition

In this section the user can define a mission profile or proceed with a default one. As shown, the user must set the final altitude for each phase and not the average one, letting to the possibility to define the cruise with variable altitude. In reality this behavior is even predicted. In fact, the control systems which manage this phase are expected to take into account the fuel consumption (and the consequent weight reduction) to follow the maximum possible efficiency pattern. In case of supersonic flight this could bring to a light increase in the altitude during cruise, reducing the drag caused by the shock wave, the surface temperature and the required thrust.

In this part of the tool the user decides which phase to define, by setting the required parameters. As it can be seen, the process is structured to give the possibility of redefining one - or more than one – phase(s), if necessary.

```
================================================================================================
|----------------------------- MISSION PROFILE DEFINITION ----------------------------|
================================================================================================

Press:

    1 => Define the mission profile
    2 => Proceed with the default mission profile

Your choice is: 1

Press:

    1 => Include the missed approach procedure
    2 => Not include the missed approach procedure

Your choice is: 1


Select the mission phase:

    1   Warm-up and taxi
    2   Take-off
    3   Subsonic climb
    4   Subsonic cruise
    5   Supersonic climb
    6   Supersonic cruise
    7   Supersonic descent
    8   Subsonic descent
    9   Final approach
    10  Missed approach
    11  Final approach (no go-away procedure)
    12  Landing
    13  Taxi-out

    0 To return to the previous menu

Your choice is: 1

---------------------------------------------
      WARM-UP & TAXI parameters definition
---------------------------------------------
Initial altitude [m]: 0
Final altitude [m]: 0
Initial speed [m/s]: 0
Final speed [m/s]: 15
Phase distance [km]: 5
Phase throttle [%]: 10
```

Figure 3.34: Mission profile definition - command window (1).

```
   WARM-UP and TAXI: confirm the values?

 Initial altitude: 0.00 m
 Final altitude: 0.00 m
 Initial speed: 0.00 m/s
 Final speed: 15.00 m/s
 Phase distance: 5.00 km
 Throttle: 10.0 %

Press 1 to confirm, 0 to modify the values.

Your choice is: 1

Select the mission phase:

    1   Warm-up and taxi
    2   Take-off
    3   Subsonic climb
    4   Subsonic cruise
    5   Supersonic climb
    6   Supersonic cruise
    7   Supersonic descent
    8   Subsonic descent
    9   Final approach
    10  Missed approach
    11  Final approach (no go-away procedure)
    12  Landing
    13  Taxi-out

    0 To return to the previous menu

Your choice is: 2


---------------------------------------------
      TAKE-OFF parameters definition
---------------------------------------------
Final altitude [m]: 30
Final speed [m/s]: 70
Phase distance [km]: 5
Phase throttle [%]: 90

    TAKE-OFF: confirm the values?

 Initial altitude: 0.00 m
 Final altitude: 30.00 m
 Initial speed: 15.00 m/s
 Final speed: 70.00 m/s
 Phase distance: 5.00 km
 Throttle: 90.0 %

Press 1 to confirm, 0 to modify the values.
```

Figure 3.35: Mission profile definition - command window (2).

The functions involved are:

- *mission_profile.mat*, the function which handles the menu and the user inputs management.
- *mission_profile_print.mat*, which manages the video print on the command window.
- *mission_profile_calculations.mat,* which performs the duration and speed calculations based on the Standard International Atmospheric (ISA) model.

In case the user selects the default mission profile, function "*mission_profile_no_user.mat"* will be run instead of the first of the list above. When the user chooses to exit the input definition section, the function *mission_profile_print.mat* is called: a table summarizing the

mission profile main parameters is printed in the command window. As reported in Figure 3.37, if the user does not confirm the mission profile, the function *"mission_profile.mat"* runs again the parameters definition, or, if it does, the function stops returning to main.

	WARM-UP & TAXI	TAKE-OFF	SUBSONIC CLIMB	SUBSONIC CRUISE	SUPERSONIC CLIMB	SUPERSONIC CRUISE
In. Altitude	0.00 m	0.00 m	100.00 m	12000.00 m	12000.00 m	18000.00 m
Fin. Altitude	0.00 m	100.00 m	12000.00 m	12000.00 m	18000.00 m	18000.00 m
In. Mach	0.04	0.04	0.29	0.80	0.88	3.00
Fin. Mach	0.04	0.29	0.80	0.88	3.00	3.00
In. Speed	0.00 m/s	15.00 m/s	100.11 m/s	272.24 m/s	299.46 m/s	1020.88 m/s
Fin. Speed	15.00 m/s	100.00 m/s	236.06 m/s	259.66 m/s	885.21 m/s	885.21 m/s
Distance	5.00 km	5.00 km	50.00 km	100.00 km	100.00 km	5500.00 km
Duration	11.1 min	1.4 min	4.9 min	6.3 min	2.8 min	98.8 min
Throttle	10.0 %	90.0 %	85.0 %	70.0 %	90.0 %	65.0 %

	SUPERSONIC DESCENT	SUBSONIC DESCENT	FINAL APPROACH	MISSD APPROACH	FINAL APPROACH	LANDING	TAXI-OUT
In. Altitude	18000.00 m	12000.00 m	2000.00 m	100.00 m	2000.00 m	100.00 m	0.00 m
Fin. Altitude	12000.00 m	2000.00 m	100.00 m	2000.00 m	100.00 m	0.00 m	0.00 m
In. Mach	3.00	0.70	0.30	0.20	0.30	0.20	0.15
Fin. Mach	0.70	0.30	0.20	0.30	0.20	0.15	0.00
In. Speed	1020.88 m/s	238.21 m/s	102.09 m/s	68.06 m/s	102.09 m/s	68.06 m/s	51.04 m/s
Fin. Speed	206.55 m/s	99.76 m/s	67.98 m/s	99.76 m/s	67.98 m/s	51.04 m/s	0.00 m/s
Distance	130.00 km	100.00 km	30.00 km	10.00 km	20.00 km	5.00 km	5.00 km
Duration	3.6 min	9.9 min	5.9 min	2.0 min	3.9 min	1.4 min	3.3 min
Throttle	50.0 %	50.0 %	40.0 %	80.0 %	30.0 %	20.0 %	10.0 %

```
-------------------------------------------
    TOTAL MISSION RANGE = 6060.00
-------------------------------------------
```

Figure 3.36: Mission profile definition - command window (results).

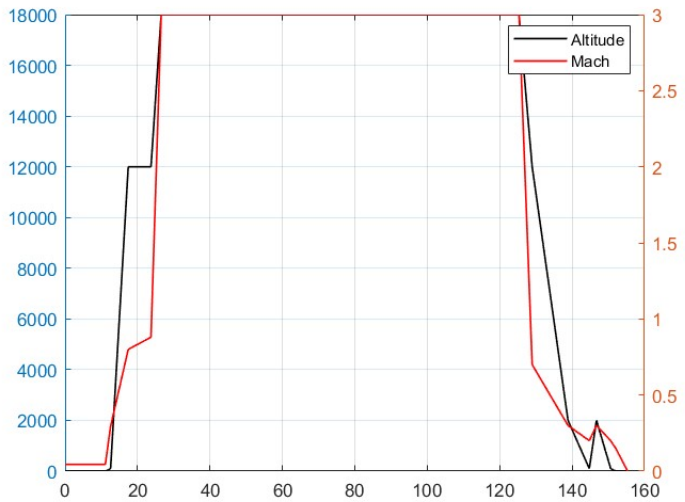

Figure 3.37: Mission profile definition results.

3.3 Weights estimation

The results of the statistical analysis and the mission profile are the inputs of the subsequent weights estimation. Following the method discussed in Section 2, an overview of the logic flow of the implemented algorithm is shown in the next diagram:

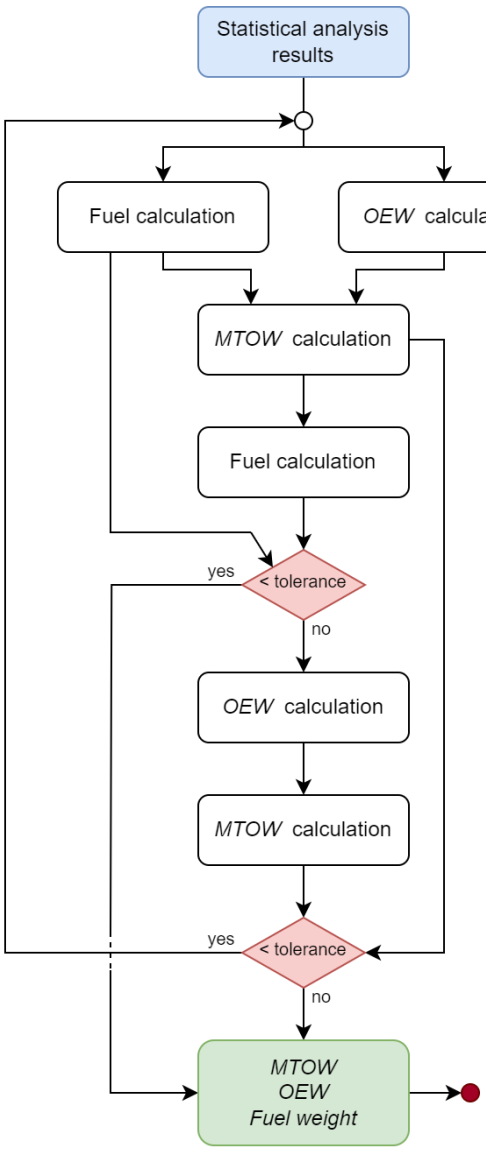

Figure 3.38: Weights estimation algorithm flow chart.

Referring to figure 3.39:

- *masses_est_Ray.mat* is the MATLAB function demanded to the implementation of the Raymer's method.

- *fuel.mat* is the MATLAB function that performs the fuel consumption through the Breguet's equation and the correction of the SFC.

Operative Empty Weight (OEW) is a fundamental factor of the total weight, which calculation is expressed through the exponential equation already discussed in Section 2:

$$\frac{OEW}{MTOW} = k_m k_{vs} \cdot A \cdot MTOW^C$$

Through this equation the Operative Empty Weight is calculated, at first using the statistical *MTOW* as input. The next step is the calculation of the fuel necessary for the mission, estimated with the Breguet's equation, in the MATLAB function *fuel.mat*:

$$\frac{W_i}{W_{i-1}} = e^{-\frac{R \cdot SFC}{V \cdot \frac{L}{D}}}$$

The Breguet's equation is applied for each phase of the mission profile defined by the user, so at the end it results in the final aircraft weight, and:

$$W_{fuel} = WMTO - W_{final} + W_{res}$$

The W_{res} term represents the fuel reserve that should be present at the end of the mission for safety purposes, i.e. multiple missed approaches, waiting circuits or different destination airport. At the end the results are passed to *masses_est_ray.mat* where the MTOW value is updated with the new fuel weight.

The whole process runs in a loop where, at each cycle, the OEW is updated with the last fuel weight and so on. Two checks are implemented in order to stop the iterations. The first one is based on the convergence of the loop: when the difference between the newest MTOW value and the previous one is smaller than a tolerance the cycle comes to an end. Otherwise, when the iteration number reaches a predefined upper limit, the same happens, meaning that the process does not reach convergence. In that case a message is shown and the tool stops:

```
    WARNING! CONVERGENCE NOT REACHED!
>>
```

Figure 3.39: Convergence not reached warning.

The needed inputs for the function to work are summarized in the next table:

Input data	
Overall efficiency	5
SFC	0.3 kg/daN/h
Engines	4
Fuel reserve	6 %

Table 3.16: Weights estimation inputs.

These data are intended to be a *first guess*. The aerodynamics calculations will provide more accurate calculations for efficiency and during the subsequent more detailed phases of the project a proper value will be obtained for the Specific Fuel Consumption as well.

At the end of the process, the outputs listed in the command window are, for this case study:

```
================================================================================
|--------------------------------- MASSES ESTIMATION ---------------------------------|
================================================================================

Set the overall aircraft efficiency ==> 5
Set the reference SFC [kg/daN/h]    ==> 0.3
Set the number of engines           ==> 4
Set the fuel reserve [%]            ==> 6

-----------------------------------------------
                  RESULTS
-----------------------------------------------
WMTO =         70785.63 kg
Fuel weight = 24520.50 kg
WOE =          37365.13 kg
WOE_WMTO =     0.53
```

Figure 3.40: Weights estimation command window.

3.4 Configuration definition

At this point the user is called to set the main geometrical features of the aircraft: it is a fundamental part because, clearly, the aerodynamic calculations depend on it. The section is complex, and the MATLAB functions involved are the following:

- *configuration.mat* is the principal function that handles the menu and calls the other ones depending on the user choices.
- *wing_profile.mat* manages the selection and draw of the wing profile.
- *check_airfoil_file.mat* controls the existence of a coordinate file and memorizes the profile coordinate.
- *wing_draw.mat* performs the wing type selection, manages the user inputs and draws the wing.
- *tail_draw.mat* manages the vertical and horizontal tail planes design and draw.
- *line_two_points.mat* calculates the leading-edge and trailing-edge representative equations, based on the geometrical data defined by the user.
- *draw_3d.mat* performs the three-dimensional draw of the aircraft configuration.
- *surf_calculations.mat* is demanded to the calculation of the wing total surface, wetted surface and volume.

In the first menu the user chose which section of the aircraft to design:

```
================================================================================
|------------------------------- GEOMETRY DEFINITION -------------------------------|
================================================================================

Press:

    1 => Define fuselage parameters
    2 => Define wing parameters
    3 => Define vertical tail parameters
    4 => Define horizontal tail parameters

    0 => Return to previous menu.
```

Figure 3.41: Geometry definition command window.

3.4.1 Fuselage

For the fuselage the data to set are the following:

- Fuselage-body length
- Fuselage mean diameter
- Nose-cone length
- Tail-cone length
- Tail-cone delta height

The last one can be set for visualization purposes only, because, to avoid tail-strike during take-off, the tail cone axis is usually deviated upwards.

Input data [m]	
Fuselage-body length	40
Fuselage mean diameter	3
Nose-cone length	10
Tail-cone length	10
Overall length	60
y-distance between LE and TE at tip station	0

Table 3.17: Fuselage geometry inputs.

```
================================================================================================
|-------------------------------- GEOMETRY DEFINITION --------------------------------|
================================================================================================

Press:

    1 => Define fuselage parameters
    2 => Define wing parameters
    3 => Define vertical tail parameters
    4 => Define horizontal tail parameters

    0 => Return to previous menu.

Your choice is: 1


------------------------------
FUSELAGE PARAMETERS DEFINITION
------------------------------

Fuselage body length [m]    ==> 40
Fuselage diameter [m]       ==> 3
Nose cone length [m]        ==> 10
Tail cone length [m]        ==> 10
Tail cone delta-heigth [m]  ==> 1

Press 1 to confirm, 0 to retry: 1
```

Figure 3.42: Fuselage geometry definition command window.

At the end of the process the following images are shown, and the user decides if continuing or starting again to change the parameters.

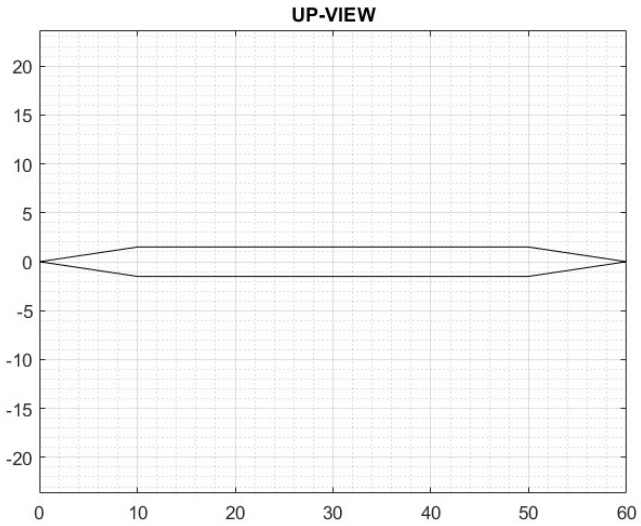

Figure 3.43: Fuselage - up view.

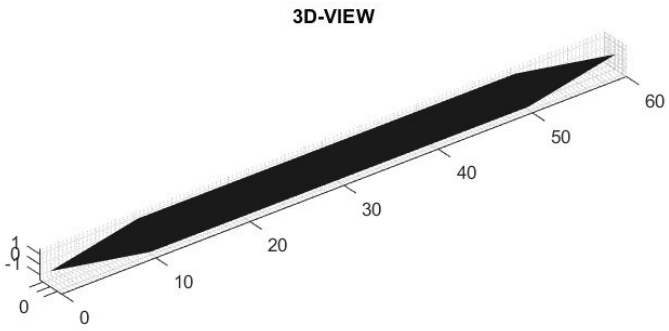

Figure 3.44: Fuselage - 3D view.

3.4.2 Wing

In this part the user set, at first, the wing profile. A database of wing profiles is already present, as shown in Figure 3.45.

```
---------------------------------------
        WING PROFILE DEFINITION
---------------------------------------

Select the wing profile:

NACA 64-series:         NACA 65-series:         NACA 66-series:

1 => NACA 64A004        9 => NACA 65-002        17 => NACA 66-004
2 => NACA 64A006        10 => NACA 65-004       18 => NACA 66-206
3 => NACA 64A008        11 => NACA 65-206       19 => NACA 66-006
4 => NACA 64A010        12 => NACA 65-010       20 => NACA 66-008
5 => NACA 64A210        13 => NACA 65-210       21 => NACA 66-209
6 => NACA 64A212        14 => NACA 65-012       22 => NACA 66-010
7 => NACA 64A015        15 => NACA 65-015       23 => NACA 66-210
8 => NACA 64A020        16 => NACA 65-020       24 => NACA 66-012
                                                25 => NACA 66-018
                                                26 => NACA 66-212

Your choice is: 4

Profile NACA_64A010.txt loaded. Press 1 to confirm, 0 to select another profile: 1
```

Figure 3.45: Wing geometry definition command window (1).

The function *Wing_profile.mat* manages the load of the file containing the selected profile normalized coordinates, the thickness to chord ratio calculation and the profile representation.

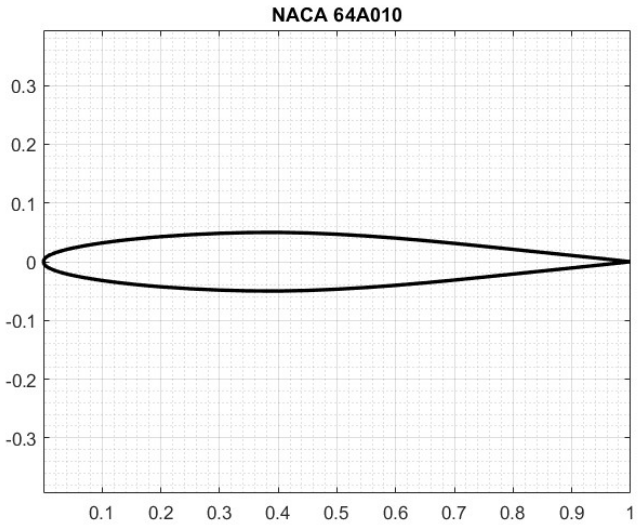

Figure 3.46: Wing profile.

If the user confirms the chosen profile, the wing definition starts with the choice of a simple or complex tapered wing. For the first option, in the function *Wing_draw.mat* one Taper Ratio only is asked to be set, while, if proceeding with the second option the values to be set are two, to define a wing with a variable sweep angle. In this case the wing can be designed to have a discrete variation or a continuous one.

As an example, the following images show the definition of a simple wing with no sweep angle variation. The input data are defined in the following table:

Input data	
Wingspan [m]	32
Root chord [m]	20
Taper Ratio	0.3
Sweep angle [deg]	55
x-coordinate of the LE at root station [m]	20
y-distance between LE and TE at tip station [m]	0

Table 3.18: Simple wing geometry inputs.

```
-----------------------------------------
        WING PARAMETERS DEFINITION
-----------------------------------------

 Press:

     1 => Simple tapered wing
     2 => Complex tapered wing

 Your choice is: 1

Simple tapered wing. Press 1 to confirm, 0 to abort: 1

 Press:

     1 => Define wing through root and tip chords.
     2 => Define wing through TR.

 Your choice is: 2


 ------------------------------
     SINGLE SWEEP WING
 ------------------------------

 Wingspan [m]            ==> 32
 Root chord [m]          ==> 20
 Taper Ratio (TR) [-]    ==> 0.3
 Sweep angle [deg]       ==> 55

 x-coordinate of the root leading edge [m]   ==> 25
 y-distance between LE and TE tip [m]        ==> 0

Press 1 to confirm, 0 to retry: 1
```

Table 3.19: Wing geometry definition command window (2).

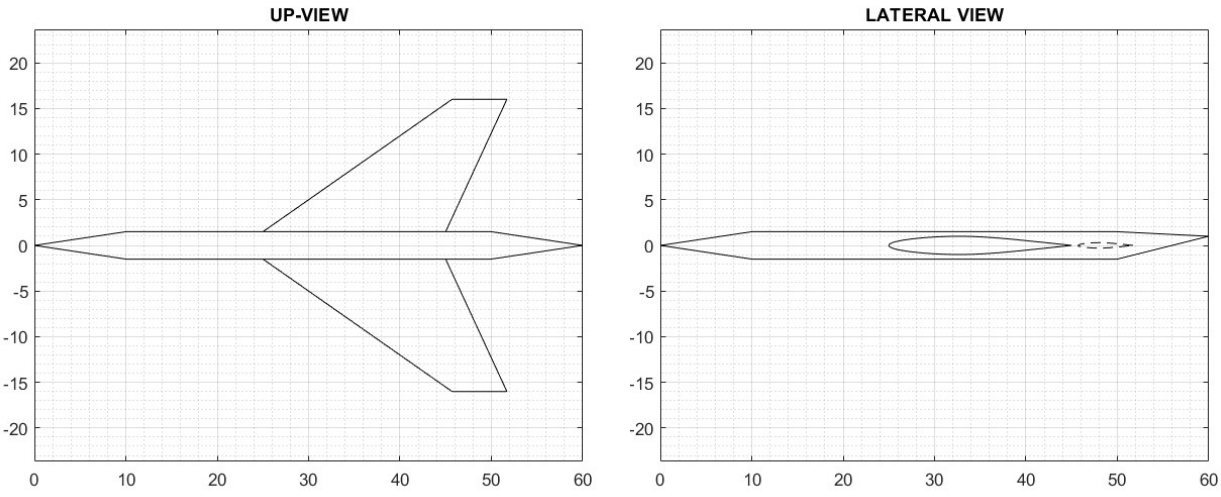

Figure 3.47: Simple wing - up and lateral view.

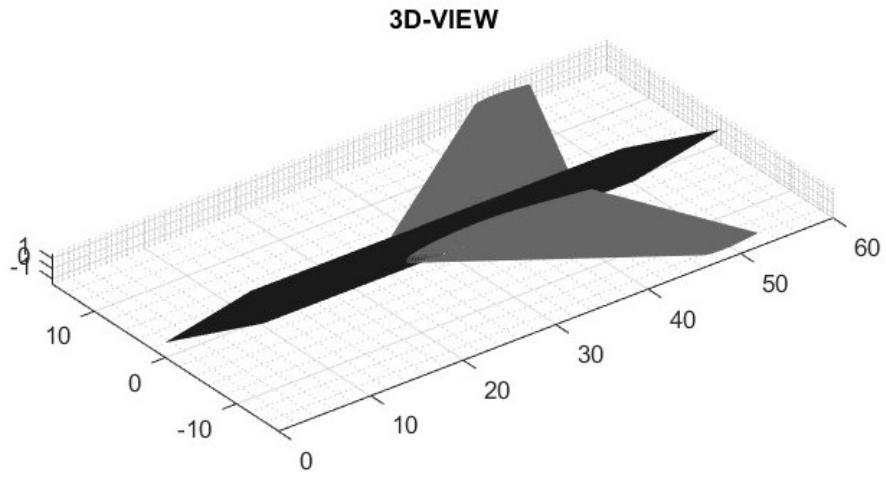

Figure 3.48: Simple wing - 3D view.

On the other hand, the following images show the definition of a complex wing with a discrete sweep angle variation, including the tail as well.

```
-----------------------------------------
        WING PARAMETERS DEFINITION
-----------------------------------------

Press:

    1 => Simple tapered wing
    2 => Complex tapered wing

Your choice is: 2

Complex tapered wing. Press 1 to confirm, 0 to abort: 1

Press:
    1 => Double sweep wing.
    2 => Continuous sweep wing.

Your choice is: 2


-----------------------------
    CONTINUOUS SWEEP WING
-----------------------------

Wingspan [m]    ==> 32
Root chord [m]  ==> 20

First Taper Ratio (TR) [-]  ==> 0.8
Second Taper Ratio (TR) [-] ==> 0.35

First Sweep angle [deg]     ==> 55
Second Sweep angle [deg]    ==> 60

x-coordinate of the root leading edge [m]   ==> 25
y-distance between LE and TE tip [m]        ==> 1

y-distance between LE and TE at second sweep station [m]    ==> 0
x-displacement of the second sweep station [m]              ==> 0

Press 1 to confirm, 0 to retry: 1
```

Figure 3.49: Wing geometry definition command window (3).

```
================================================================================
|-------------------------------- GEOMETRY DEFINITION --------------------------------|
================================================================================

Press:

    1 => Define fuselage parameters
    2 => Define wing parameters
    3 => Define vertical tail parameters
    4 => Define horizontal tail parameters

    0 => Return to previous menu.

Your choice is: 3


------------------------------
        VERTICAL TAIL
------------------------------

Wingspan [m]    ==> 4
Root chord [m]  ==> 5

Taper Ratio (TR) [m]    ==> 0.3
Sweep angle (deg) [m]   ==> 50

x-coordinate of the root leading edge [m]   ==> 48

Press 1 to confirm, 0 to retry: 1

================================================================================
|-------------------------------- GEOMETRY DEFINITION --------------------------------|
================================================================================

Press:

    1 => Define fuselage parameters
    2 => Define wing parameters
    3 => Define vertical tail parameters
    4 => Define horizontal tail parameters

    0 => Return to previous menu.


Your choice is: 4


------------------------------
        HORIZONTAL TAIL
------------------------------

Wingspan [m]    ==> 4
Root chord [m]  ==> 5
Taper Ratio (TR) [m]    ==> 0.3
Sweep angle (deg) [m]   ==> 50
x-coordinate of the root leading edge [m]   ==> 48

Press 1 to confirm, 0 to retry: 1
```

Figure 3.50: Wing geometry definition command window (4).

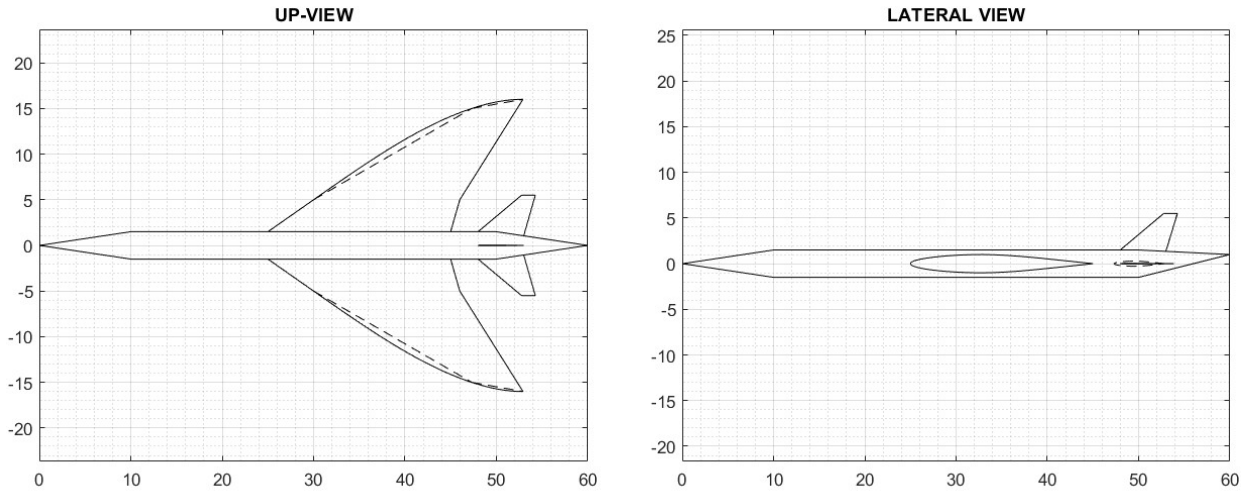

Figure 3.51: Complex wing - up and lateral view.

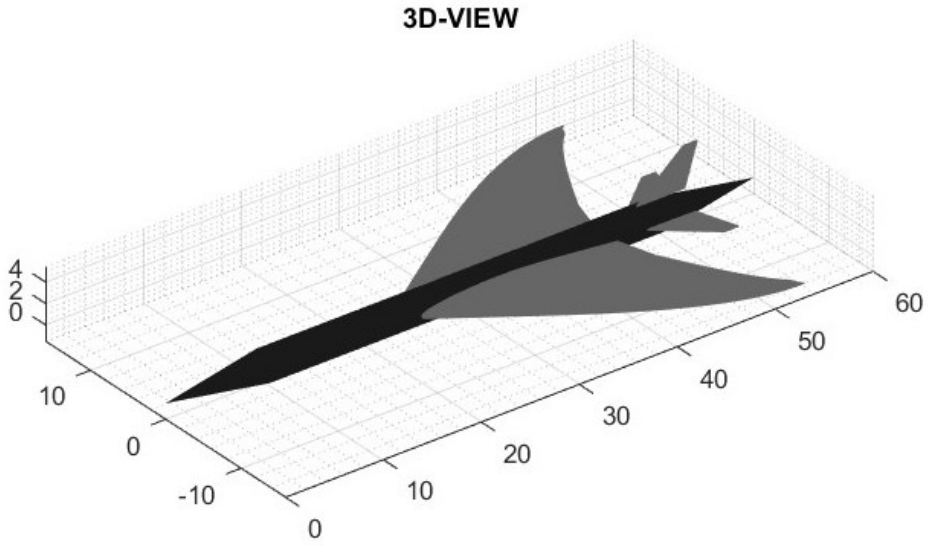

Figure 3.52: Complex wing - 3D view.

In the first two images the equivalent simple wing is shown dashed. If the user selects the continue sweep angle option, the function asks for two values for every parameter and, at the end, the results are interpolated. In this case the image shows a comparison between the continue sweep wing and the equivalent discrete one. Normally the second option is chosen because in the supersonic regime all abrupt variations should be avoided. Moreover, this could lead to a decrement in the structural resistance of the wing.

At the end of the process, the images are updated with the presence of the wing and the function *draw_3d.mat* performs the three-dimensional visualization. The Aerodynamic Mean Chord is also calculated, together with the section and volume distributions across the wingspan, the total and wetted surface and the total volume of the wing.

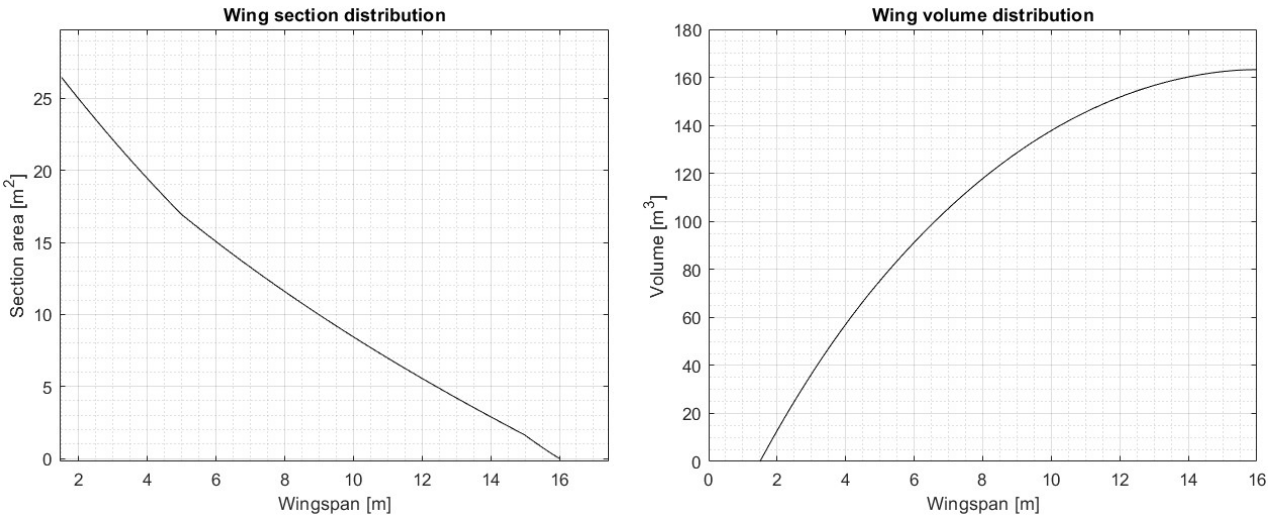

Figure 3.53: Wing section and volume distributions.

The calculations are made through integrations based on the points coordinates of the profile.

$$x_p = x_{TE} + x_{p,ad} \cdot c(y)$$

$$y_p = y_{TE} + y_{p,ad} \cdot c(y)$$

$$dV = (S_i + S_{i+1}) \cdot \frac{(y_{i+1} - y_i)}{2}$$

If the *x-axis* is the longitudinal one and the *y-axis* is parallel to the wingspan, x_p and y_p are the dimensional coordinate of the point at position y of the semi-wingspan, $x_{p,ad}$ and $y_{p,ad}$ are the dimensionless coordinate of the profile extrapolated from the function *wing_profile.mat*, $c(y)$ is the chord at station y of the wingspan and x_{TE} is the position along the *x-axis* of the trailing edge.

For this case study, the following values were found:

Output data	
Wing surface	323.73 m^2
Wing wetted surface	707.45 m^2
Total wetted surface	1215.5 m^2
Aspect ratio	3.16
SMC wing	11.05 m

Table 3.20: WIng geometry definition outputs.

3.4.3 Tail

For what concerns the tail, in the function *tail_draw.mat* the same logic as the wing definition is implemented, both for the horizontal and vertical plane. Here the user can define simple tapered surfaces only, not necessarily both: as a matter of fact, it is a common choice to design only the vertical one for supersonic vehicles, as the Concorde, with the presence of flaperons and ailerons to compensate for the lack of control surfaces on the vertical plane. However, with the main purpose of showing the tool working and logic flow, in this case of study have both been set.

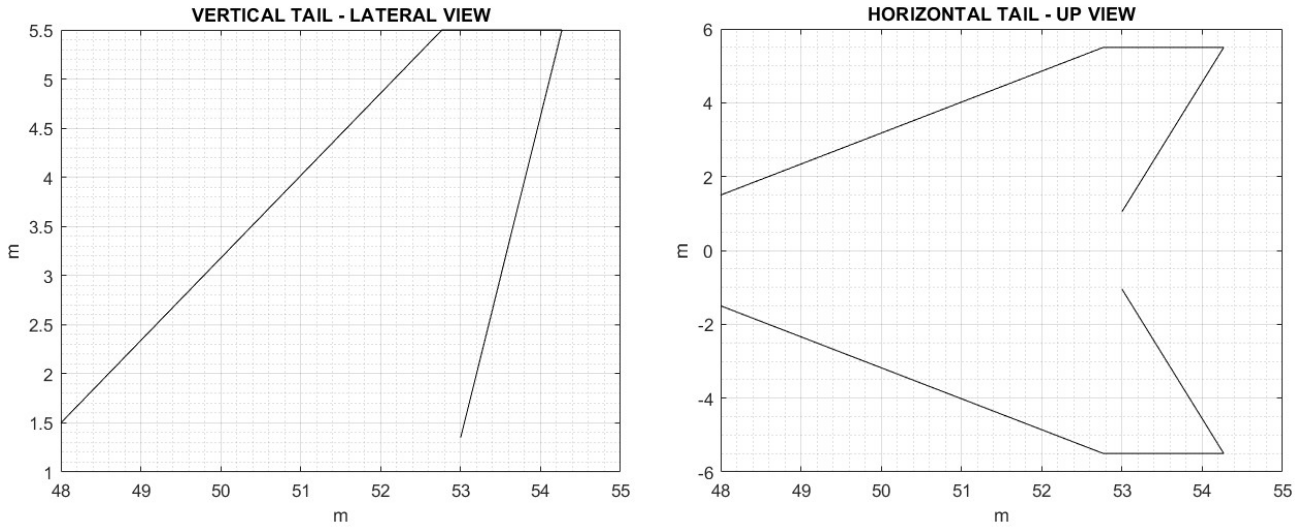

Figure 3.54: Tail geometry - lateral and up view.

3.5 Aerodynamics

For the aerodynamic calculations all the geometrical features defined in the previous section are needed as input of the functions:

- *Raymer_aero.mat*, which manages the input and output data.
- *Raymer_calculations.mat* implements all the theories detailed in Section 2.3.2.
- *cruise_drag.mat* is colled by the *main* and calculates the total drag developed during the supersonic cruise.
- *polar.mat* defines the wing polar graphs.

Within the function *Raymer_calculations.mat* the two matrixes C_L and C_D are the outputs, with the two aerodynamic coefficients expressed in their dependance of the flight Mach and angle of attack. Those functions also run in a loop varying the flaps deflection between the discrete values of 0°, 5°, 15° and 25°. However, the increase in lift is computed only through the increase in the wing surface, while the drag increase takes place within the Miscellaneous drag term, according to the equation:

$$C_{D,misc,basearea} = \frac{\left(0.139 + 0.419(M - 0.161)^2 \cdot S_{flap}\right)}{S_{exp}}$$

This equation has already been detailed in Section 2.3.2. In the figure below the command window is shown.

```
================================================================================
|----------------------------------- AERODYNAMICS -----------------------------------|
================================================================================

Press:

    1 => Perform analytical calculations (Raymer)
    2 => Show reference results from CFD analysis

Your choice is: 1
```

Figure 3.55: Aerodynamics - command window.

During development of the algorithm, CFD results from a *Mach 2* case were taken as reference[30], and the results were transposed to be coherent with the case study through the equations:

$$C_{L_{case-study}} = \frac{C_{L_{CFD}}}{S_{wing_{case-study}} / S_{wing_{CFD}}} \cdot \frac{S_{wet_{case-study}}}{S_{wet_{CFD}}}$$

$$C_{D_{case-study}} = C_{D_{CFD}} \cdot \frac{S_{wing_{CFD}}}{S_{wing_{case-study}}}$$

The database contained also the contribution for the flaps deflection. The results are summarized below.

M	$\alpha\,[deg]$	$\delta_{FLAP}\,[deg]$	C_L	C_D
0.3	0	0	0.02	0.01
0.3	0	5	0.06	0.01
0.3	5	0	1.42	0.07
0.3	5	5	1.50	0.11
0.3	7	15	1.88	0.17
1.2	0	0	0.10	0.15
3	0	0	0.02	0.06

Table 3.21: Aerodynamics results - CFD database [30].

On the other hand, the results of the analysis, according to the design choices already made in the previous sections, are summarized below:

M	$\alpha\,[deg]$	$\delta_{FLAP}\,[deg]$	C_L	C_D
0.3	0	0	0.04	0.03
0.3	0	5	0.08	0.07
0.3	5	0	1.69	0.09
0.3	5	5	1.74	0.13
0.3	7	15	2.13	0.20
1.2	0	0	0.13	0.16
3	0	0	0.03	0.11

Table 3.22: Aerodynamics results - Raymer model.

These values appear consistent with the ones found in literature. Moreover, through the lift coefficient calculated for the cruise phase it is possible to find the Lift force:

$$L = \frac{1}{2}\rho_{CR} V_{CR}^2 S \cdot C_L$$

And, comparing it with the aircraft weight force at the beginning of the cruise:

$$L - W \cdot g = -4.774 \cdot 10^3\ N$$

This difference can be reduced by increasing the angle of attack, which is usually done during cruise. Moreover, the aircraft weight reduces during the mission. These results appear to be consistent with the ones obtained from the CFD calculation. At the end of the process, the function *Cruise_drag.mat* performs the calculation of the drag developed during the supersonic cruise and the available thrust, correcting the one received from the statistical analysis with the already detailed equation:

$$T = \phi * \varphi * T_{ref}$$

$$\phi = \frac{\Pi_{phase}}{\Pi_{cruise}} \qquad \varphi = \frac{p_{phase}}{p_{sl}}\left(\frac{T_{sl}}{T_{phase}}\right)^{1.75}$$

$$D = \frac{1}{2}\rho_{CR}V_{CR}^2 S \cdot C_D$$

$$D - T_{Max} = -1.56 \cdot 10^3$$

It is a fundamental step to set the power system requirements and the average throttle during cruise phase. Within the next development of this tool, the possibility to calculate them for all the mission phases can be implemented as, being a high-level feasibility analysis, at this early stage it has been preferred not to deepen the detail level due to the high uncertainties of the main parameters.

It is evident that the developed drag during the supersonic cruise is higher than the maximum available thrust at the cruise altitude chosen. At this point, two “paths” can be followed to try to make the available thrust enough to perform the supersonic cruise:

- Interrupt the process and start the design process all over again, changing the geometrical features to reduce the developed drag.
- Accepting the lack in thrust and pursue with the analysis: the needed thrust-to-weight ratio will be highlighted after the requirement verification section and the new thrust

requirement may be set as input of a second iteration run of the tool, instead of the one computed by the statistical analysis.

The increase in the number of engines may also be made, but an increase in the miscellaneous and interference terms of the drag should be taken into account. Also, a decrement in the cruise altitude should result in a higher available thrust, as the increase in the atmospheric density would play a positive contribution. On the other hand, the drag may increase and the engines may change their work design point. Anyhow, such an analysis is necessary to set the engines requirements.

3.6 Wing polar charts

At the end of the configuration definition, the user has the possibility to plot three important curves, necessary to summarize the bond intercurrent between the two aerodynamic coefficients, the angle of attack and the Mach number.

- $C_L - \alpha$: it shows the variation of the lift coefficient with respect to the angle of attack value.
- $C_L - C_D$: it represents the aerodynamic polar, describing the variation of the lift coefficient with respect to the drag coefficient.
- $C_L - Mach$: it shows the dependence of the lift coefficient on the Mach number. Within the used model, this graph should consider the effects of the transonic and supersonic regimes as well.
- $E - Mach$: it shows the wing efficiency variation with the Mach number.

The MATLAB function *polar.mat* only requires the two aerodynamic databases created before. As shown in the image below, the user only needs to enter the Mach number and the angle of attack value.

```
================================================================================
|---------------------------------- WING POLAR ----------------------------------|
================================================================================

Enter the Mach number   ==> 0.7
Enter the AoA value [deg]   ==> 1

Press 1 to confirm, 0 to plot again the graphs  ==>
```

Figure 3.56: Wing polar charts - command window.

The example here presented is the subsonic case, which could be the case of the subsonic cruise phase of the mission.

M = 0.7

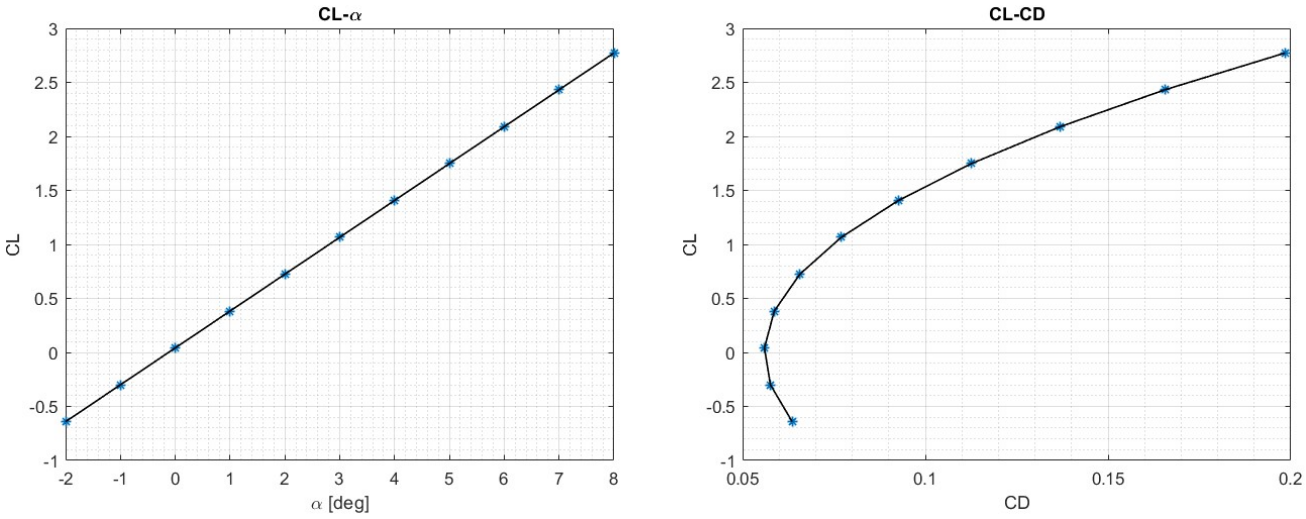

Figure 3.57: C_L-α and aerodynamic polar curves (Mach = 0.7).

As expected, the lift coefficient increases linearly with the angle of attack, while the aerodynamic polar presents the typical shape with the concavity facing downwards. In this graph C_L and C_D are considered at fixed Mach number and varying angle of attack, so that smaller α values correspond to small C_L and C_D coefficients. In these conditions, small variations in the C_D correspond to large variations in the C_L. On the contrary, larger C_L and C_D values are typical of larger α values and under these conditions, larger variations in the C_D correspond to smaller variations in the C_L.

The next graphs show the C_L and the efficiency trends with the Mach number at fixed angle of attack, set equal to 1° to emulate the conditions during a subsonic cruise. Also, at 0° the lift coefficient may be near equal to zero, even for light asymmetrical wing profiles, thus leading to numerical errors during calculations.

α = 1°

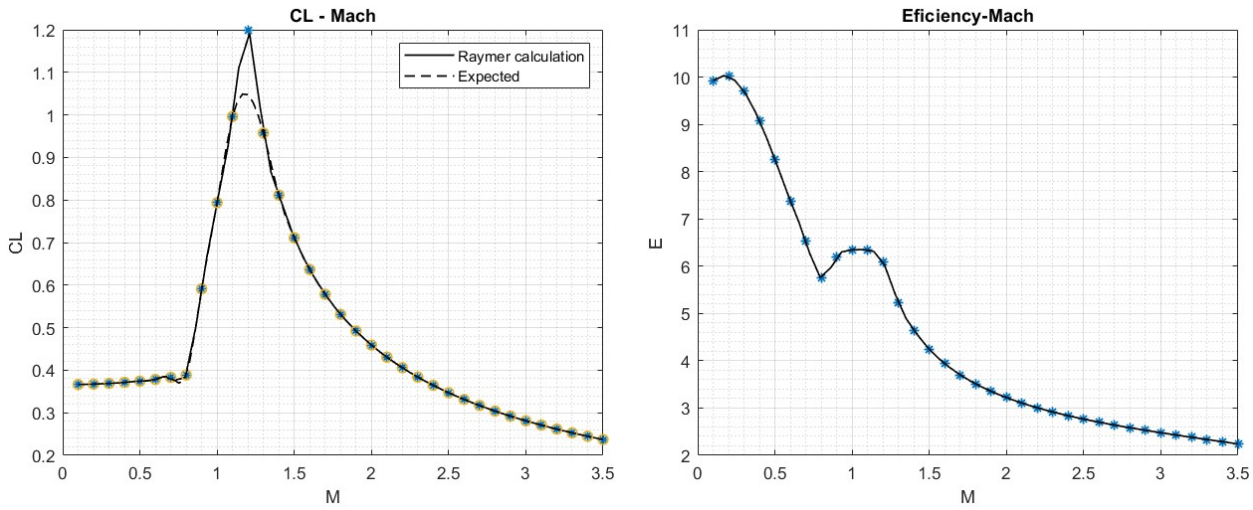

Figure 3.58: C_L-Mach and Efficiency-Mach curves (α = 1°).

In the first one is evident the increase in the C_L when entering the transonic regime of flight, typical behavior caused by the increase in the air compressibility, followed by a rapid decrement. The peak is around $M = 1.2$, as reported in tables 3.21 and 3.22. The decreasing trend is due to several factors, but mainly to the formation of shock waves which cause the drop of the flow speed downstream of the shock itself, so the flow, as the Mach number increases, reaches the wing surface at increasingly lower speeds. Moreover, even if the wing design and materials are such to minimize the flow separation, this phenomenon could in part occur so that the positive effect of the profile camber is lower. All these aspects also have the effect of increasing the drag coefficient, explaining the behavior shown in the efficiency-Mach graph.

3.7 Requirements verification

3.7.1 Take-off and landing requirements

With the set of equations, representing the mathematical transposition of the CS-25[13] requirements in matter of take-off and landing phases, the function *to_lan.mat* performs the calculation of the Take-off speed, the take-off required minimum distance, the landing speed and the landing minimum required distance. As shown in the next image, the results are available to the user in the command window.

```
================================================================================
|-------------------------------- TAKE-OFF & LANDING --------------------------------|
================================================================================

TAKE-OFF distance:  836.77 m
TAKE-OFF speed:     52.34 m/s

LANDING distance:   1254.92 m
LANDING speed:      44.61 m/s
```

Figure 3.59: Take-Off and landing requirements verification - command window.

Of course, these results depend on all the previous ones, thus, in case of unsatisfactory results, the best option may be to start all over the whole process. In the case study example, it was chosen to go on.

3.7.2 Performances requirements verification: matching chart

The performances requirements verification[10] is the ultimate output of the high-level feasibility study, where results from the statistical analysis, masses estimation, overall configuration and aerodynamics calculations all converge. All the equations discussed in Section 2 are implemented in the MATLAB function *matching_chart.mat*, where all the needed parameters are set and not available for the user to modify during the program execution. Table 3.23 summarizes them.

Set data	
Vertical speed during climb	1200 ft/m
Instantaneous turn - load factor	1.26
Sustained turn – load factor	1.5
Instantaneous turn altitude	1000 m
Sustained turn altitude	1000 m
Angle of attack during cruise	0 deg
C_L during instantaneous turn	$0.9 \cdot C_{L_{Max}}$
Instantaneous turn rate	3 deg/s
Oswald factor	0.8
Minimum climb gradient	0.3

Table 3.23: Matching charts input data.

Given the peculiarities of the supersonic flight regime, it was chosen to separate the analysis for the subsonic and supersonic phases. Two matching charts will be provided: the user should set the two ratios $\frac{T}{W}$ and $\frac{W}{S}$ in accordance with the most stringent requirement.

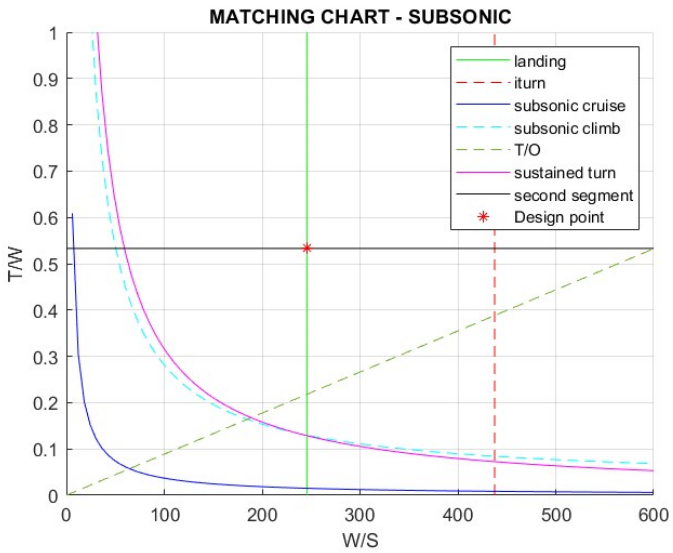

Figure 3.60: Matching chart - subsonic case.

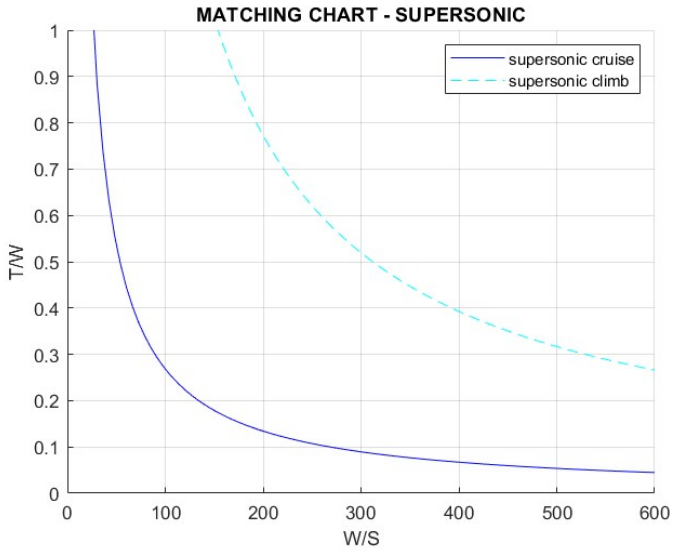

Figure 3.61: Matching chart - supersonic case.

The ultimate output of the case-study feasibility analysis with the definition of the two ratios. The following could be likely values:

$$\frac{T}{W} = 0.53$$

$$\frac{W}{S} = 246\ \frac{kg}{m^2}$$

These results can be used as input of a second iteration, through the calculation of the thrust and wing surface:

$$T = 0.53 \cdot MTOW = 385\ kN$$

$$S = MTOW/246 = 288\ m^2$$

The results are also shown in the command window:

```
=========================================================================================
|---------------------------------- MATCHING CHART ----------------------------------|
=========================================================================================

Design point as resulted from the Matching Chart:

|---------------|-----------------------|
|   T/W = 0.53  |   Thrust = 385 kN     |
|---------------|-----------------------|
|   W/S = 246   |  Wing Surf. = 288 m2  |
|---------------|-----------------------|
```

Figure 3.62: Matching chart - command window.

The whole analysis was conducted taking as reference one of the airplanes from the statistical database, the Boom Overture. The choice fell on this, rather than on the others, because of the similar main features and because, being the operative phase predicted in 2029, it represents the state-of-the-art of the modern, sustainable, supersonic commercial aviation.

It must be noted that such an approach acts as a validation of the algorithm in its entirety. In every section of the tool the case study presented within this document as an example, all the inputs required were chosen to be similar to the counterparts of the Boom Overture. Working with this data set, the tool "creates" a concept-aircraft with comparable features with the Boom Overture itself. In the following table this consideration is highlighted, with the case-study output data reported in green.

	Case-study		**Boom Overture**
Passengers	70		72
MTOW	70786 kg		77111 kg
Propellant weight	24520 kg		38600 kg
PMF	0.53		0.50
Cruise Mach	3		1.7
Range	6060 km		7870 km
Thrust	385 kN		356 kN
Wing surface	As resulted after configuration.mat	324 m^2	218 m^2
	As resulted after matching_chart.mat	288 m^2	
Wingspan	32 m		32.3 m
Length	60 m		61.2 m
W/S	246 kg/ m^2		354 kg/ m^2

Figure 3.63: Case study and Boom Overture comparison [21].

SECTION 4

Conclusions and boundaries of application

The aim of this thesis is to show that it is possible to formulate a coherent model which, with the definition of several inputs, can perform a high-level feasibility analysis of a modern supersonic commercial aircraft. Moreover, the Mach 3 case can give a smoother path for developing practical applications like commercial supersonic travel and a deeper understanding of how to handle the increasingly severe aerodynamic and thermal challenges as speeds approach the hypersonic threshold.

Given the theoretical nature of the algorithm, the obtained results are not presumed to faithfully represent the ultimate features of the final product, even after a second iteration using the final outputs as the new inputs. However, taking advantage of empirical correction factors to get the models closer to reality and convergence loops, the algorithm capabilities have been proved, as shown in Table 3.64.

A sensitivity analysis was performed in order to define the tool's boundaries of applicability whit respect of the variation of the three main high-level requirements: passengers' number, cruise Mach and total mission range. The MATLAB code was run to obtain all the combinations of the three variables within the following ranges:

- Passengers' number between 50 and 120.
- Mach number between 2 and 4.
- Range between 5000 km and 7000 km.

The behavior can be summarized in the graphs below.

The Maximum Take-Off Weight trend is a direct consequence of the Fuel Weight one: if the mission range increases, they both increase, while the opposite occurs when the Mach number increases. This is due to the formulation of the Breguet's equation, with the speed at the denominator of the fraction, so that if the speed increases the weight ratio decreases, taking account of the fact that the time duration of the cruise phase decreases. However, the formulation of fuel consumption doesn't consider the variation of the *SFC* with the speed, because it's a specific parameter of the engine, which is unknown at this stage.

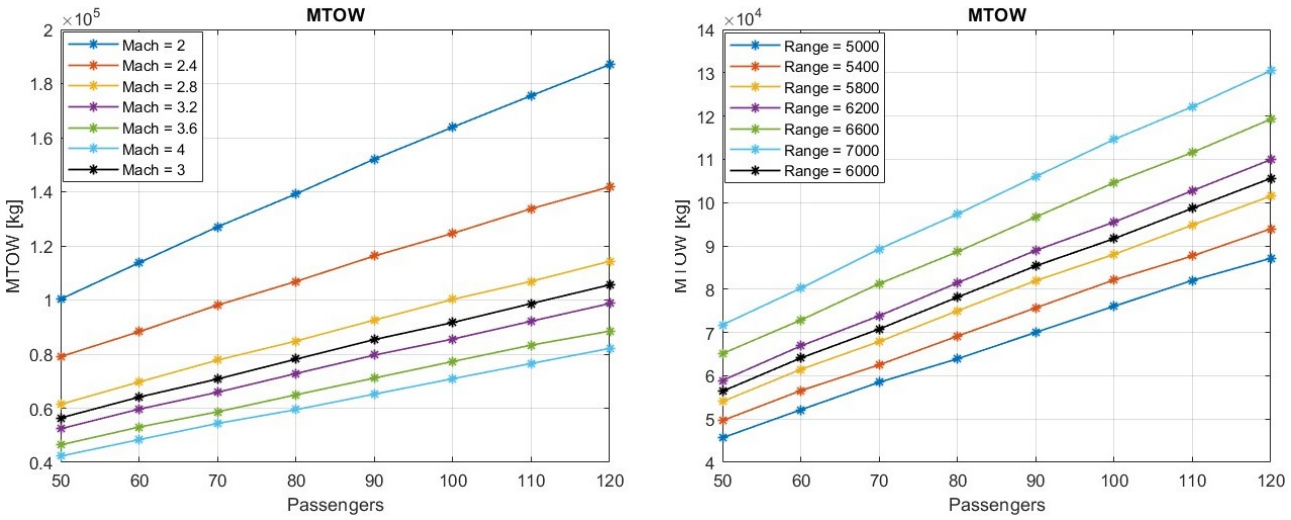

Figure 4.1: Sensitivity analysis with respect to payload, MTOW and range.

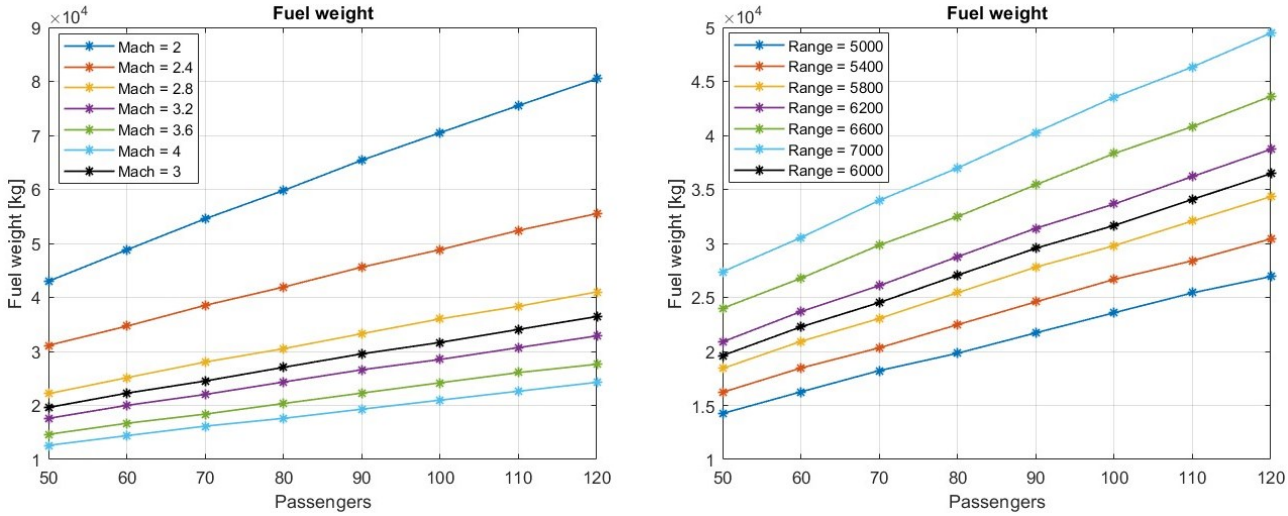

Figure 4.2: Sensitivity analysis with respect to payload, fuel weight and range.

During the iterations, the convergence was monitored, and it showed some instabilities for every combination that satisfies the conditions:

$$M \leq 2.2$$

$$Range > 6500\ km$$

While the passengers' number doesn't appear to be a critical factor (given the note on the fuel consumption), around 60% of the combination within the two values above caused the rise of the convergence alert flag:

```
WARNING! CONVERGENCE NOT REACHED!
>>
```

Figure 4.3: Convergence not reached warning.

Another trend of interest is the Wing Loading one which, according to the figures, shows a very low sensitivity to the payload variation. This is because, given that the corrections of the geometrical features were made through fixed values, the weight and the wing surface vary accordingly. Such an explanation may not be true at low Mach and high range where the trends diverge, so these results are not reliable.

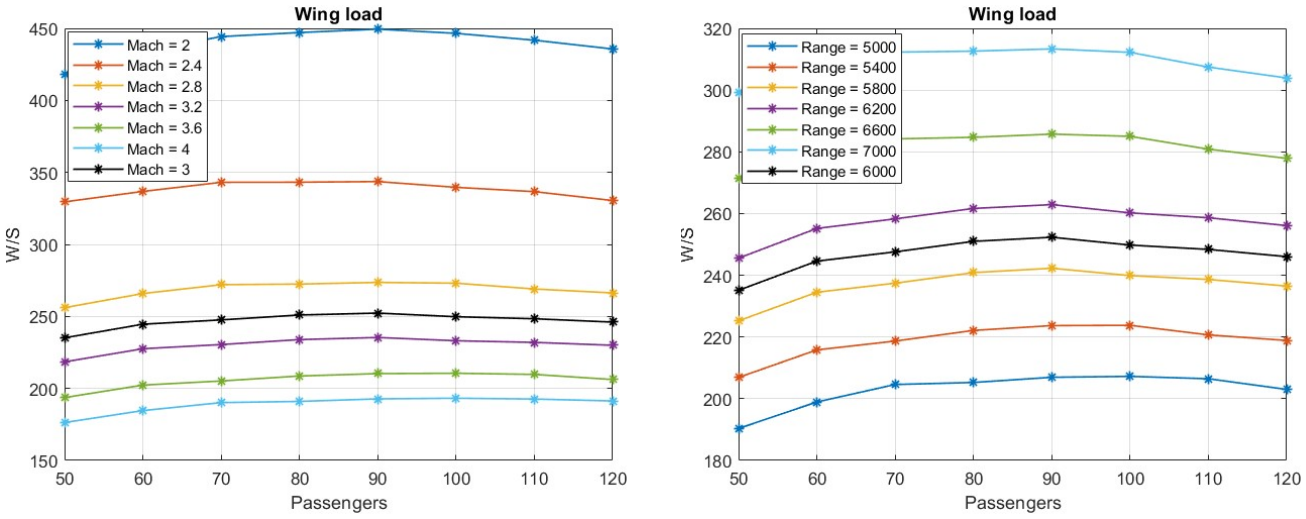

Figure 4.4: Sensitivity analysis with respect to payload, wing load and range.

Given the reliability of the algorithm and its limitations, some updates could be made to improve the quality of calculations. Firstly, the selection of the engine or its design, even at low level of definition, would allow us to set more accurate inputs for the weights estimation.

Moreover, the acknowledge of the real engine performances would lead to a realistic setting of the throttle, improving the fuel consumption calculations, together with the SFC correction for the speed.

The tool handles the wing surface and volume calculations through integrations based on the point coordinates of the profile and this data could be used for preliminary dimensioning and allocation of the fuel tanks. This would lead to the stability analysis for which the masses distribution definition is a requirement. However, the total volume enclosed by the wing surfaces is a gross estimation of the real available volume, due to the presence of the structural elements and their definition is beyond the purposes of this work.

Another field of improvement is the aerodynamics calculations for what regards the wing profile, which could include the calculation of the camber for the definition of the zero-lift angle of attack for asymmetrical profiles, which was made manually.

List of figures

List of tables

References

1. Federal Aviation Administration, *Transport Airplane Accident Library - Air France Flight 4590*, F-BTSC, 2000.
2. United Nations, *Framework Convention on Climate Change. Conference of the Parties, Twenty-first session,* 2015.
3. Eurocontrol, *Seven-year flights service units forecast 2018-2024*, 2018.
4. EUROCONTROL, *Aviation outlook 2050 report*, 2022.
5. Boeing, *Commercial Market Outlook*, 2024. https://cmo.boeing.com/
6. European Commission*, MDO and REgulations for Low-boom and Environmentally Sustainable Supersonic aviation*, 2021. https://cordis.europa.eu/project/id/101006856/results
7. POLIFLASH ARCHIVE, *MOREandLESS: towards the future of civil supersonic aviation,* 2021. https://archivio-poliflash.polito.it/en/research_innovation/moreandless_towards_the_future_of_civil_supersonic_aviation
8. ICAO, *Resolution A39.1 Consolidated statement of continuing ICAO policies and practices related to environmental protection – General provisions, noise and local air quality.*
9. G. Piccirillo, R. Fusaro, D. Ferretto, et al. *MORE&LESS Task 6.1 - Progress meetings*, 2023.
10. Nicole Viola, Roberta Fusaro, Davide Ferretto, et al. *Integrated Aerospace System Design, course lessons*, A.Y 2024.
11. Egbert Torenbeek, *Essentials of Supersonic Commercial Aircraft Conceptual Design*. 1st ed. Wiley; 2020.
12. Daniel P. Raymer. *Aircraft Design: A Conceptual Approach*. Sixth edition. American Institute of Aeronautics and Astronautics, Inc; 2018.
13. EASA, *Certification specifications and acceptable means of compliance for large aeroplanes (CS-25).*
14. Sukhoi T-4. In: *Wikipedia*. https://en.wikipedia.org/w/index.php?title=Sukhoi_T-4&oldid=1245551748
15. TUPOLEV Tu-444. https://janes.migavia.com/?view=article&id=1237:tu-444
16. Aerion SBJ. In: *Wikipedia*. https://en.wikipedia.org/w/index.php?title=Aerion_SBJ&oldid=1244923468
17. SAI Quiet Supersonic Transport. In: *Wikipedia*. https://en.wikipedia.org/w/index.php?title=SAI_Quiet_Supersonic_Transport&oldid=1258390593
18. *SAI resurrects QSST-X as all-first class supersonic airliner, seeks investors.* https://avtales.wordpress.com/2013/06/12/sai-resurrects-qsst-x-as-all-first-class-supersonic-airliner-seeks-investors/
19. Spike S-512. In: *Wikipedia*. https://en.wikipedia.org/w/index.php?title=Spike_S-512&oldid=1218340585

20. *Aerion e la NASA insieme per il futuro del volo supersonico civile e commerciale. Aviation Report.* https://www.aviation-report.com/aerion-e-la-nasa-insieme-per-il-futuro-del-volo-supersonico-civile-e-commerciale/
21. Boom Overture. In: *Wikipedia*. https://en.wikipedia.org/w/index.php?title=Boom_Overture&oldid=1257324143
22. Boom - Overture. Boom. https://boomsupersonic.com/overture
23. Concorde. In: *Wikipedia*. https://it.wikipedia.org/w/index.php?title=Concorde&oldid=141895691
24. Tupolev Tu-144. In: *Wikipedia*. https://it.wikipedia.org/w/index.php?title=Tupolev_Tu-144&oldid=141106869
25. Boeing 2707. In: *Wikipedia*. https://it.wikipedia.org/w/index.php?title=Boeing_2707&oldid=140255073
26. North American XB-70 Valkyrie. In: *Wikipedia*. https://en.wikipedia.org/w/index.php?title=North_American_XB-70_Valkyrie&oldid=1257848907
27. Lockheed L-2000. In: *Wikipedia*. https://en.wikipedia.org/w/index.php?title=Lockheed_L-2000&oldid=1256255875
28. Leading Aerospace and Defense. Lockheed Martin. https://www.lockheedmartin.com/en-us/index.html
29. Tupolev Tu-244. In: *Wikipedia*. https://en.wikipedia.org/w/index.php?title=Tupolev_Tu-244&oldid=1245115849
30. Roncioni P., Marini M., Gori O., Fusaro R., Viola N., *Aerodatabase Development and Integration and Mission Analysis of a Mach 2 Supersonic Civil Aircraft*, 2024.